Mapping Post-Harvest Transportation Losses in Vegetable Quality: Retrieval of Environmental Conditions and their effect on In-Cargo Tomato Quality Using Remote Sensing Techniques and Geographic Information Systems

by

Daniel Kwabena Asare-Kyei

Thesis submitted to the International Institute for Geo-information Science and Earth Observation and Kwame Nkrumah University of Science and Technology in partial fulfilment of the requirements for the degree of Master of Science in Geo-information Science and Earth Observation, Specialisation: (GIS for Natural Resource Management).

Thesis Assessment Board

Prof. Dr. Ir. E.M.A Smaling, (ITC, Chairman)
Dr. B. K. Prah, (Rector, Kumasi Polytechnic, External Examiner)
Prof. Samuel K. Oppong (First internal examiner, KNUST)
M r. J. A. Qyaye-Ballard (Second internal Examiner, KNUST)
Ir. Louise M. van Leeuwen (Course coordinator, ITC)

Supervisors: Msc Valentijn Venus (ITC), Prof. Samuel Oppong (KNUST), Mr. J. A. Quaye-Ballard (KNUST)

INTERNATIONAL INSTITUTE FOR GEO-INFORMATION SCIENCE AND EARTH OBSERVATION
ENSCHEDE, THE NETHERLANDS
KWAME NKRUMAH UNIVERSITY OF SCIENCE AND TECHNOLOGY KUMASI, GHANA

Disclaimer

Abstract

The dynamics of in-cargo environmental conditions and vegetable quality are important to predict the future quality evolution of tomatoes in transit as influenced by temporal variability of climatic conditions. This study aims to develop models that predict in-cargo micro-climate in relation to temporal variability of outside environmental conditions and assess how the in-cargo micro-climate relates to the quality of tomatoes during transportation. In-cargo and outside climatic conditions were measured with data loggers every 15 minutes to coincide with a satellite overpass time during the transportation of tomatoes within Ghana. The General Estimating Equations (GEE) models developed to predict the in-cargo micro-climate integrate the temporal variability of outside climatic conditions with geo-referenced and remotely sensed determinants of Land Surface Temperature (LST) and radiation for the entire road corridor. Tomato firmness was evaluated with a fruit pressure tester (penetrometer) and the quality evolution modelled using analytical equations for steady state conditions. The results showed that the in-cargo micro-climate varies linearly with the outside environmental conditions except the LST which was non-linear. The GEE model yielded accurate and unbiased predictions for the in-cargo temperature and relative humidity (RH). The variance explained for the in-cargo temperature was 77% at a RMSE of 4.18^{0}C whilst that of the in-cargo RH was 84% at a RMSE of 19.59%. The model however, failed to give sensible results for the in-cargo light intensity. The quality evolution model explained 77% of the firmness variance. It was established that the firmness of tomatoes decreased exponentially during transportation with a reference rate constant of 0.0075hour^{-1} (1.25 X 10^{-4}/min) and activation energy of 20.411KJmol^{-1}. Also the average estimated firmness of the simulations at any trajectory of the predictor variables was 0.96 ±0.53Kg. The results showed the possibility of using GIS techniques to map the quality of tomatoes continuously in time and space throughout transportation. The approach presented to predict the in-cargo micro-climate; and the models formulated to estimate and map the tomato quality losses under various scenarios of environmental conditions; appear to be promising tools in the management of the post-harvest chain and open new frontiers in the application of remote sensing and GIS in post-harvest quality studies.

Keywords: In-cargo micro-climate, environmental conditions, General Estimating Equations, Tomatoes, Open Trucks, Transportation, Post-harvest loss, Firmness, Quality evolution modelling, Quality map, Remote sensing, GIS-based regression mapping.

Acknowledgements

In the first place, I wish to express my profound gratitude to the almighty God for his guidance, protection and love over the years that have brought me to this level and also, to the management of ADRA Ghana, especially our Country Director, Mr. Samuel Asante-Mensah for nominating me and providing the necessary support for my studies. Special appreciation goes to my immediate supervisor, Mr. Tony Augustus Mainoo for his inspiration and guidance since I joined the organization. Also, I am grateful to ITC for providing the funds for this important course.

My heartfelt gratitude goes to my supervisors; M.Sc. Valentijn Venus, Prof. S. K. Oppong and Mr. J. A. Qyaye-Ballard for their advice, sound criticisms and incredible commitment to the cause of this study. Special thanks go to my own friend Tyn, for his tolerance and readiness to share a lot of his knowledge throughout the thesis period. I enjoyed working with you.

I am thankful to Prof. Pol Tijskens of the Horticultural Supply Chains, Wageningen University for providing direction in certain aspect of the study. Also, special thanks to Prof. Dr. E. M. A Smaling, Dr. David Rossiter, M.Sc. Bas Wesselman and Ir. Louise van Leeuween for their pieces of advice especially, during the proposal development phase. Mr Seth Adjei Fosu, a tomato farmer at Tuobodom, your crucial role during the data collection has not been forgotten. Many thanks to all truck drivers and tomato traders whose cooperation has been key to the success of this work

My profound appreciation also goes to all GISNATUREM (Kumasi) and NR students (Enschede) of 2007-2009 especially, Ruben Venegas and also Gerald Fourkuo for your diverse contribution to this work.

Lastly, to my sweet wife, Comfort and beloved son, Chief; the entire Asare-Kyei family; my special friend, Nana Ama Acheampong; my business partner and friend, Kwasi Etu-Bonde, I express my gratefulness for the support, patience, encouragements and motivation you gave me which kept me going throughout the difficult times.

May God bless you all!

Table of contents

List of figures

List of tables

List of Equations

1. Introduction

1.1. Background

Despite the remarkable advances made in increasing food production at the global level, approximately half of the population in the third World do not have access to adequate food supplies (FAO, 1989). There are many reasons for this, one of which is food losses occurring in the post-harvest and marketing system. The report suggests that these losses tend to be highest in those countries where the need for food is greatest (FAO, 1989). There are several accounts on the estimate of post-harvest losses in developing countries. A study conducted by New Agriculturist (2005) estimated post-harvest losses to be anywhere between 20- 100%. In the light of growing demand for food and land resources, such losses are simply unacceptable.

In West Africa, vegetables are transported in open trucks and the use of improved post-harvest technology is largely unavailable. If West African agriculture is to be improved, then the proper understanding of the dynamics of vegetable quality during transportation is critical. This assertion is buttressed by the fact that competitiveness in African agriculture could be enhanced by good post-harvest management practices (FAO, 2004). Studies show that reduction in the post-harvest loss, particularly if it can economically be avoided, would be of great significance to growers and consumers alike (FAO, 1989). Also, it can reduce the rate of deforestation caused by agricultural land expansion.

Causes of post-harvest quality loss vary widely. All fruits and vegetables are living plant parts and contain 65 to 95% water. They continue their living processes after harvest. Their post-harvest life depends on the rate at which they use up their stored food reserves and their rate of water loss (FAO, 1989). When food and water reserves are exhausted, the produce dies and decays. Thus, it is clear that any factor that increases the rate of this process will reduce the quality of the vegetables. It is not yet known how the factors causing loss in vegetable quality plays out for tomatoes under dynamic condition of transportation. Part of this study thus concerns modelling the decay of tomato firmness during transportation.

Climatic factors, in particular Land Surface Temperature (LST), Relative Humidity (RH) and light intensity (solar radiation), greatly have impact on the post-harvest quality of vegetables. Temperature is said to be the most important environmental factor that influences the deterioration of harvested produce. Relative humidity can influence water loss, decay development, the incidence of some physiological disorders, and uniformity of fruit ripening (FAO, 2004). In growing plants, optimal temperature is maintained by transpiration processes. However, organs isolated from the plant lack this protective effects of transpiration and direct sources of heat, such as sunlight, can rapidly elevate the temperature of tissues to a point above the thermal death point of their cells, leading to localized bleaching, necrosis (sunburn or sunscald) or general collapse (FAO, 2004). Light intensity is therefore an important climatic factor to consider in modelling quality losses of vegetables in the West African sub region where transported vegetables are subjected to direct radiation because of the use of uncovered trucks. The effect of wind speed on vegetable quality has been explained by FAO (1989) as follows. The faster the surrounding air moves over fresh produce the quicker water is lost. It is therefore likely that the increased air movement generated by the speeding trucks will have detrimental effects on the quality of the vegetables.

Most of the physical, biochemical, microbiological and physiological reactions contributing to deterioration of produce quality are largely dependent on temperature. Metabolic processes including respiration, transpiration and ripening are particularly temperature-reliant. Generally, rates of biological reactions increase by a factor of 2 or 3 for each 10°C increase in temperature (Beaudry *et al.*, 1992; Exama *et al.,* 1993). Also Lana *et al.* (2005) found out that the firmness of tomato decreases exponential during storage. This obviously suggests there is a strong non-linear relationship between the post-harvest quality of tomatoes and the weather conditions (micro-climate) within which they are transported or stored as well as the duration of transport. Moreover, these reviews illustrate the many studies that have been done on the physiology of harvested vegetables but firmness losses associated with open transportation system in the West African sub region is not well understood.

A number of studies on post-harvest quality evolution of vegetables especially for tomato have been developed. Examples include Lana *et al.* (2005), Lana *et al.* (2006), Lukasse & Polderdijk (2003), and Schouten, *et al.*, (2007). However, studies which couple this physiological quality modelling with the dynamics of in-cargo environmental conditions and vegetable quality are lacking. Such important information needed to predict the future quality evolution as a function of temporal variability of climatic conditions of tomatoes in transit still remains largely unknown. Qiao *et al.* (2005) argues that though produce quality is a significant factor that affects market value of crops, it has not received much attention as compared to yield.. The concept of information-aided agricultural products especially for high class vegetables such as tomatoes is classified with information on quality, harvesting time and location (Qiao *et al.*, 2005). Therefore, Quality maps are just as important as quantity maps.

Recently, remote sensing has been used to estimate these weather conditions (radiation, land surface temperature and relative humidity) with a higher temporal resolution and high coverage than that provided by ground data (Mueller *et al.*, 2004; Stisen, *et al.*, 2007; Yang *et al.*, 2006). Many algorithms have been developed to estimate these environmental conditions from real time remotely sensed data. For temperature alone, Cumba (2006) reported that three major algorithms are available. These are mono-window, split window and multi-angle methods. The mono-window method can be applied when a single thermal channel is available, though it gives the least accuracy. The Split window method uses two channels of NOAA-AVHRR and compensates for atmospheric water vapour but however requires emissivity retrieval approach. The Multi-angle method works with advance sensors and allow for the separation of component temperatures.

For solar radiation, the use of HELIOSAT method (Hammer *et al.*, 2003) based on radiative transfer model is widespread. These methodologies have been widely used in crop growth models, weather forecasting and vegetation studies and their application to post-harvest vegetable quality studies is virtually non-existent. For instance, Mostovoy *et al.* (2006) reported that remotely sensed land surface temperature has been amply used for field and regional scale estimates of the surface heat flux for weather prediction and that much experience has been gained in this area. Again, Doraiswamy *et al.* (2004) used this methodology to improve yield prediction mapping by applying leaf Area Index (LAI) estimates from MODIS surface spectral reflectance measurements and by assimilating these estimates into a crop simulation model.

The entire procedure followed by the present study has been categorized into three main tasks. These are:

i. Application of remote sensing techniques comprising of the 4 Channel Split window algorithms (Sun & Pinker, 2007) for the estimation of Land Surface Temperature (LST) and the HELIOSAT-3 method (Hammer *et al.*, 2003) to estimate incident solar radiation along the transportation corridor.
ii. Development of a model to relate the remotely sensed estimated variables to predict the in-cargo micro-climate. In-cargo micro-climate is defined here as prevailing environmental conditions of temperature, light intensity and relative humidity inside the trucks or the tomato crates. The General Estimating Equations (GEE) model will be used here and its robustness in simulating the in-cargo micro-climate will be assessed. The GEE is an empirical model developed by Liang & Zeger (1986).
iii. Development of tomato quality (firmness) evolution model to determine and map the quality of the vegetable in a GIS environment. A non-linear optimization analysis by way of analytical equations will be used here. Use will also be made of non-linear regression and the Inverse Distance Weighted (IDW) interpolation scheme. Details on non-linear regression analysis can be found in Moore *et al.* (2009).

From the reviews in paragraphs 4 and 5, firmness of tomatoes can be deduced to be a function of the in-cargo micro-climate and the duration after harvest.

Firmness = *f* (temperature + relative humidity + light intensity + time)

Modelling the in-cargo environmental conditions in relation to temporal dynamics in the ambient climatic factors and relating it to the quality of the vegetables will be a novel application of these remote sensing, bio-statistical and GIS techniques. It will also provide a better understanding on how ambient environmental conditions influence the micro-climate in the trucks and how that translate into quality losses of vegetables in the West African vegetable marketing chain. Knowledge of such a system is essential for the proper management and improvement of the West African vegetable marketing chain and will serves as the basis for the application of remote sensing and GIS techniques in Ghana in particular and the entire West African sub-region where the use of these technologies is limited.

1.2. Research Problem

As vegetables are transported from a major producing area in Burkina Faso to Accra in Ghana by trucks for both domestic consumption and export, quality losses are unavoidable. The duration of the transport, road conditions and in- cargo environmental conditions all influence the quality of the vegetable. This is because factors affecting post-harvest food losses of perishables vary widely from place to place and increasingly become complex as systems of marketing become more complex (FAO, 1989). The complexity of the marketing function relating to transportation leads to unavoidable quality losses especially in West Africa where post-harvest technologies are largely absent (FAO, 2006). Though the use of Modified Atmosphere Packaging (MAP), evaporative cooling system and refrigerated trucks have been proven to result in quality optimization and a reduction in post-harvest loss (Fonseca *et al.*, 2002), these technologies are largely unavailable in Burkina Faso and Ghana and often vegetables are transported in open trucks.

Figure 1-1 Open transportation system used in West Africa (left) compared with a refrigerated truck (right) in high-technology countries.

This type of transportation in Figure 1-1 (left), undoubtedly, will results in substantial monetary losses and its concomitant rise in poverty levels in the study area where FAO (1989) estimate that between 20-40% of harvested crops are lost due to poor post-harvest handling. Extensive literature review yielded no results on the dynamics of environmental processes associated with such a transportation system and the resultant loss in vegetable quality along the post-harvest chain. Knowledge of the trucks' micro-climate is thus essential for proper management and improvement of the post-harvest chain. Also efficient post-harvest systems are particularly important because as competition for land and water increase and, with migration of rural people to urban areas, there are likely to be less farmers producing food for more consumers (New Agriculturist, 2005).

Despite the importance of integrating these climatic conditions with quality evolution, the number of studies in which temperature and relative humidity have been coupled is limited (Paull, 1999). Fortunately, remote sensing allows for the estimation of these variables with high temporal resolution than that provided by point measurements (Mueller *et al.*, 2004). In particular, the METEOSAT Second Generation (MSG) satellite series with its Spinning Enhanced Visible and Infrared

Imager (SEVIRI) gives new possibilities for measuring top of atmosphere radiances and reflectance at spatio-temporal resolutions of 3km and 15 minutes respectively (Schroedter-Homscheidt *et al.*, 2008). This possibility has not been explored in post-harvest quality studies. Using estimates of these environmental variables from real time remotely sensed images; it should be possible to construct a model that predicts the micro-climate in the trucks used to transport the tomatoes. Besides, the driving application of this work will be to predict the quality of tomatoes along the entire transportation chain.

1.3. Research Objectives

1.3.1. General Objective

The broad objective is to develop a model that predicts the in-cargo micro-climate in relation to temporal variability of outside environmental conditions and assess how the in-cargo micro-climate relate to the quality of tomatoes during transportation.

1.3.2. The Specific objectives

The specific objectives of the study are:

- To determine the relationships between in-cargo micro-climate and outside environmental conditions including remotely sensed estimates of Land Surface Temperature (LST) and solar radiation
- To develop a model that integrates temporal variability of in-cargo micro-climate, outside environmental conditions and their geo-referenced determinants of LST and solar radiation in predicting in-cargo micro-climate using the General Estimating Equations (GEE) model.
- To model and determine the dynamic quality evolution of the tomato in relation to the temporal variability of the in-cargo micro-climate.
- To test the sensitivity of tomato firmness decay to the in-cargo micro-climate
- To map the quality of the tomato along the transportation corridor using GIS-based regression mapping approach.

1.4. Research Questions

The study will strive to address the following questions:

- How dynamic are these environmental factors of temperature, RH, radiation, and wind speed; and how do they influence the micro-climate in the trucks?
- Is it possible to apply the General Estimating Equations (GEE) model to accurately predict the in-cargo micro-climate?
- To what extent does the changing in-cargo micro-climate affect the firmness (quality) of the tomatoes being transported?
- How sensitive is the tomato quality to fluctuations in the in-cargo micro-climate?

1.5. Hypotheses

The following hypotheses have been formulated for the research questions. Some of the research questions have more than one hypothesis. For instance, the hypothesis for question 1 has been sub-divided into 3. The sub-level hypotheses are in bullets.

1. In-cargo micro-climate is linearly related to the outside environmental conditions as follows:
   - In- Cargo Temperature = f (Land Surface Temperature, Outside air temperature, Wind Speed)
   - In-cargo Relative humidity = f(Tomato skin temperature, outside air temperature, outside Relative humidity)
   - In-cargo light intensity = f(Solar Radiation)
2. The GEE model can estimate the model parameters with reasonably accurate standard errors and hence the predicted parameters will have confidence interval of higher coverage rates.
3. The changing in-cargo micro-climate under such a transportation system can lead to significant exponential losses in the tomato quality.
   - The quality of the tomatoes under such a transportation system depends largely on the in-cargo micro-climate and the duration after harvest.

On model validations, it is further hypothesized that for the model to be free from systematic error and be considered a perfect predictor, then the following null hypotheses must hold:

In-cargo micro-climate:

H_o: intercept = 0 and H_o: slope $\beta_1 = \beta_2 = \beta_n = 1$. The alternate hypothesis is:

H_a: intercept ≠ 0 and Ha: slope $\beta_1 \neq \beta_2 \neq \beta_n \neq 1$.

Where β_1, β_2, β_n are the slopes of the predictor variables, x_1, x_2, x_n.

Quality evolution model:

Ho: $\beta = 1$ and

Ha: $\beta \neq 1$

1.6. Research Approach

As elaborated in section 1.1, three main tasks were undertaken during this study. LST and solar radiation were initially estimated from MSG images in the Integrated Data Viewer (IDV) after extensive literature review. This was followed by the application of GEE models to fit the in-cargo micro-climate models. Analysis of Variance (ANOVA) and the Two Samples T-test were also used to describe the distribution of the data. Thereafter, the tomato quality evolution model was developed using analytical solutions and then actual mapping of the in-cargo micro-climate and tomato quality loss was done. The results were presented and discussed simultaneously. For a detail understanding of the research approach see Figure 1-2 for the various set of methodology used to answer the research questions.

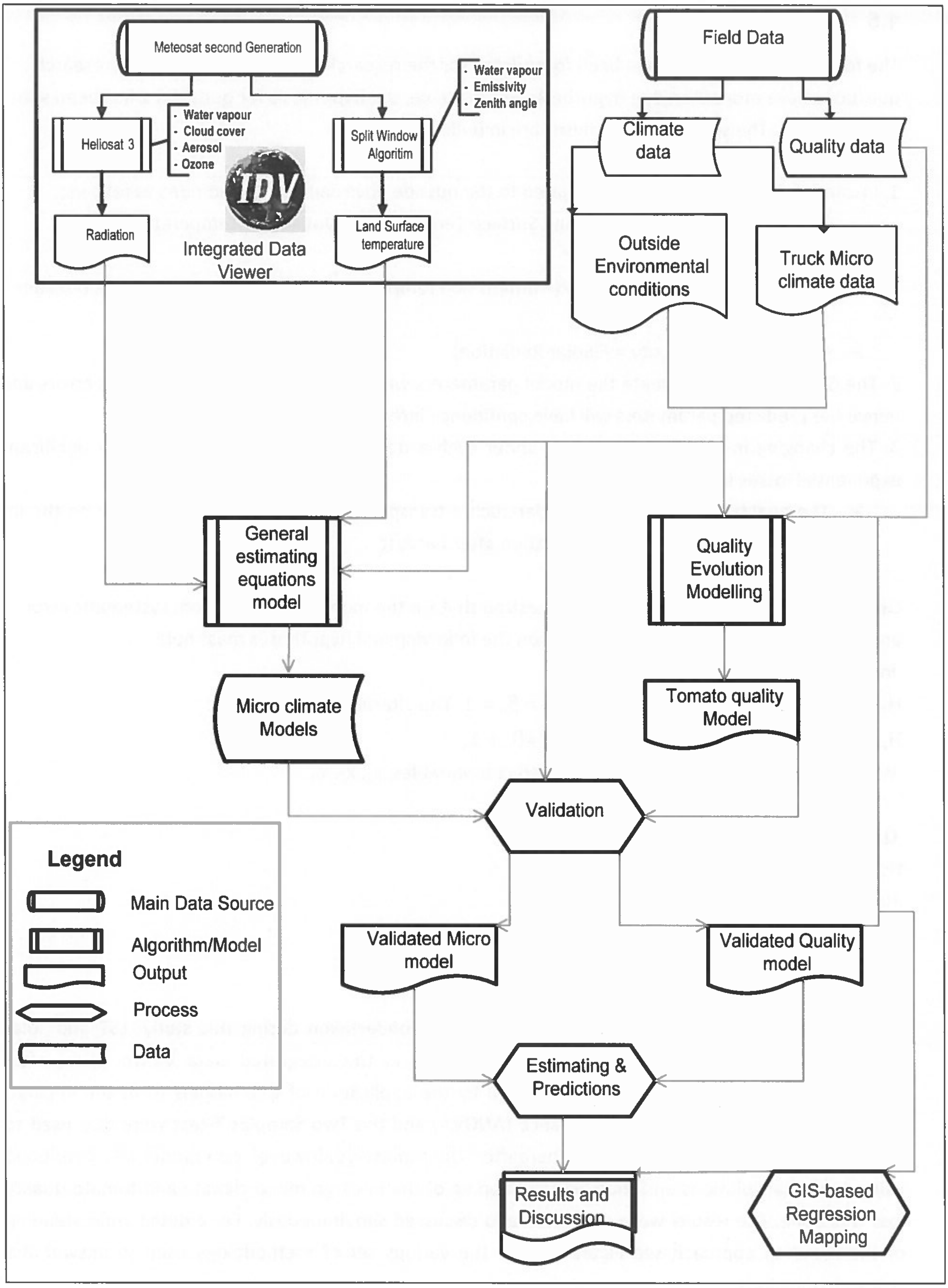

Figure 1-2 Schematic representation of study approach

2. Concepts and Definitions

2.1. Post-harvest Loss and Quality Indicators

Postharvest loss is a "measurable quantitative and qualitative loss of a given product at any moment along the postharvest chain" (De Lucia & Assennato, 1994); and includes the change in the availability, edibility and wholesomeness of the food that Prevents it from being consumed (FAO 1989). Post-harvest losses are highest with horticultural produce like tomatoes whose post-harvest quality is much dependent on climatic conditions.

Quality is defined as the composite of product characteristics that offers value to the buyer or consumer (De Lucia & Assennato, 1994) or more loosely as "the degree of excellence of a product or its suitability for a particular use" (Abbott, 1999). There are several quality attributes of fresh produce. However, for the purpose of this study, one of these quality attributes, firmness of tomatoes will be assessed. Firmness is a textural attribute of vegetables defined as the ratio between pericarp, locular tissue, and skin toughness (Ali, 1998). According to Ali (1998) and Mizrach (2008), it is among the factors widely considered in quality assessment, is used for commercial quality expectations and is easily measured. Firmness is considered as a good indicator of the quality of vegetables (Lana *et al.*, 2005). Understanding how this quality attributes changes after harvesting is thus fundamental to establish good management practices in the agricultural industry and during distribution and marketing. Modelling the firmness of fruits and vegetables as an indication of the overall quality has been done in many studies. Examples include Ali (1998), Lana *et al.* (2005), Mizrach (2008), Schouten *et al.* (2007) and Van Dijk *et al.* (2006).

2.2. Significance of Post-harvest loss to Natural Resource Managment

High post-harvest losses mean that vegetable farmers in West Africa have to expand the land area under cultivation from season to season to compensate for the anticipated losses. This practice of continued expansion of farm land is exerting more pressure on the natural resource base. For example FAO (2006) reported that there is widespread nutrient depletion of soils arising from continuous cropping. The over-exploitation of forest resources for food production is a major cause of deforestation and loss of biodiversity throughout the sub-Saharan region and post-harvest loss has been found to contribute significantly to deforestation.

2.3. Climatic Factors Affecting Post-harvest Quality of vegetables

It has been reported that ripe tomato can be stored for a relatively longer period provided conditions are favourable, notably a temperature and relative humidity of 10–15°C and 85–95%, respectively (Castro *et al.*, 2005). Studies by Getinet *et al.* (2008) also proved that maintaining relatively lower temperature and higher relative humidity during storage using evaporative cooling systems could maintain the quality of tomato. Again, Yeshida *et al.* (1984) indicated that high temperature increases enzymatic catalysis and leads to biochemical breakdown of compounds in fruit and vegetables. Getinet *et al.* (2008) further concluded that the marketability of tomatoes was improved by 84.4% when tomato fruits were stored under evaporatively cooled storage for 16 days. Temperature and relative humidity are two major criteria used to define critical limits in monitoring programs associated with the hazard analysis and critical control point (HACCP) system (Paull, 1999). HACCP, a preventive quality assurance system, is required so that safety programs regarding deterioration of harvested produce during transportation are properly implemented.

Figure 2-1 shows the relationship between temperature and (a) day length within which the quality of vegetables can be retained (b) the rate of deterioration of quality expressed as ripening rate. Studies by Tano *et al.* (2007) also revealed that temperature fluctuations encountered during transportation and storage of fresh fruit and vegetables has a considerable impact on produce quality.

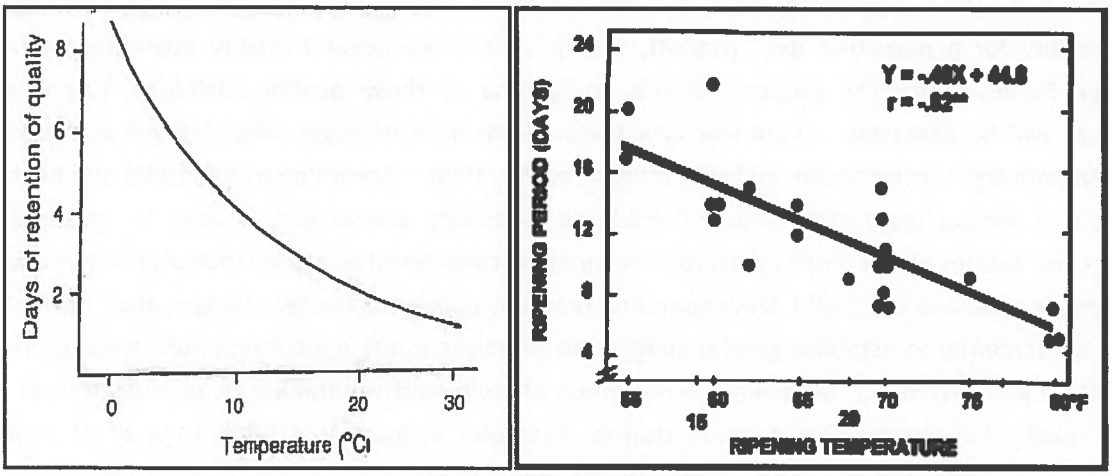

Figure 2-1 Relationship between temperature and tomato quality
(a) Relationship between temperature and quality retention period (b) Relation between temperature and rate of deterioration: Source: Ryall & Lipton (1979) Cited In: (AVRDC, 2006)

2.4. METEOSAT Second Generation/SEVIRI

For more than 40 years, meteorological satellites have provided the best way to observe the changing weather on a large scale. METEOSAT is a geostationary satellite in the equatorial plane at an altitude of 36,000 kilometres above the Earth. The drawback of the relatively high altitude is that it limits spatial resolution. The first of the new generation of METEOSAT satellites, known as METEOSAT Second Generation (MSG), was launched in August 2002 from the Kourou in French Guiana. The satellite's 12-channel imager, known formally as the spinning enhanced visible and infrared imager (SEVIRI), scans the full disk of the Earth with an unparalleled repeat cycle of 15 minutes in 12 spectral wavelength regions. Raw data coming from the SEVIRI instrument are pre-processed at EUMETSAT headquarters in Darmstadt, Germany. The eight thermal IR and three solar channels have a spatial resolution of three kilometres at nadir and scan the full disk of the Earth. The high-resolution visible channel provides images with one kilometre sampling at nadir (EUMETSAT, 2006).

2.5. Remote Sensing Algorithms

The improved thermal channels of the SEVIRI sensor have been tested by Peres & DaCamara (2004) who used simulated MSG/SEVIRI data for the retrieval of surface temperature and emissivity. Sun & Pinker (2007) compared the new four channel split window algorithm with the SP Split window algorithm (Sun & Pinker, 2003) and BL local split window algorithm developed by Becker & Li (1990) and concluded that the new algorithm "gives results closer to observations" than the generalized split window algorithms. More importantly, Cumba (2006) applied the algorithm in the study area proposed for this work and found that the 4 channel LST algorithm can be used with enough confidence to estimate LST with r^2 of 82%.

With the launch of the METEOSAT Second Generation (MSG) satellite, the possibilities for monitoring the Earth's atmosphere have improved enormously. These capabilities, Mueller *et al.* (2004) agreed; have allowed for the retrieval of additional atmospheric parameter. Several computational methods have been developed in the last two decades for the estimating of downward solar irradiance. For instance, Yank *et al.* (2006) classified these empirical methods into: sunshine based models, cloud based models and temperature based models. The HELIOSAT method belongs to the cloud based models and it is one of the best methods currently available (Mueller *et al.*, 2004). Zelenka *et al.* (1999) as well as Perez *et al.* (1998) reported that METEOSAT satellite data could be converted by the HELIOSAT method into irradiance with better accuracy than interpolated ground measurements could provide. A derivative of this algorithm called HELIOSAT-2 has been optimized as an operational processing chain for climatological data (Lefe`vre *et al.*, 2002). The HELIOSAT-2 method has been refined into HELIOSAT-3 and it exhausts the enhanced capabilities of MSG (SEVIRI). The accuracy of the calculated irradiance has increased significantly; the calculation method is now faster, accurate and provides spectrally resolved solar irradiance data (Mueller *et al.*, 2004). This study will make use of the Heliosat 2-3 approach to take advantage of the enhanced performance.

2.6. General Estimating Equations Model

Generalized linear models (McCullagh & Nelder, 1983), an example of empirical (statistical) model have been used to analyse independent observations and a variety of discrete and continuous outcomes (Zeger *et al.*, 1988). However, when the observations are correlated and time dependent as expected from the repeated observations of the variables in the truck, there is the need to use a more robust empirical technique. The General Estimating Equations (GEE) model (Zeger & Liang, 1986) used to model the in-cargo micro-climate could integrates the temporal variability of in-cargo environmental conditions and their geo-referenced determinants of land surface temperature (LST) and solar radiation at each point along the transportation route.

Recently, it became obvious that spatial autocorrelation is often present in bio-geographical datasets (Carl & Kühn, 2007). This means that observations closer to each other are more likely to be similar than those far apart. One therefore could have a lack of independence in a dataset. When repeated observations are made on a subject, correlation is anticipated among the subject measurements and must be accounted for to obtain a correct statistical analysis. The General Estimating Equations

Model was developed by (Zeger & Liang, 1986) to handle correlated data. This method has been used in several studies. For instance, Smargiassi *et al.* (2008) used GEE to develop a model that predicts in-door temperature in an urban setting. Also Carl & Kűhn (2007) used GEE to account for spatial autocorrelation in species distributions in Germany and concluded that it produces sensible results than the Generalized Linear Models (GLMs).

2.7. Energy Exchanges in Tomato Trucks

Porter *et al.* (1973) originally developed a heat balance of a terrestrial ectotherm which they expressed as a function of incoming energy from different sources: direct, scattered and reflected solar radiation; sky and ground thermal radiation; metabolic heat and air temperature; and losses from conduction, convection and evaporative cooling. This balance can also be subjective to other biophysical parameters such as are wind speed (at ground level) and or environmental humidity. This is a challenge taken by the present study to assess how these factors interact to affect the in-cargo micro- climate. The modified biophysical model has been schematic represented as shown in Figure 2-2 below.

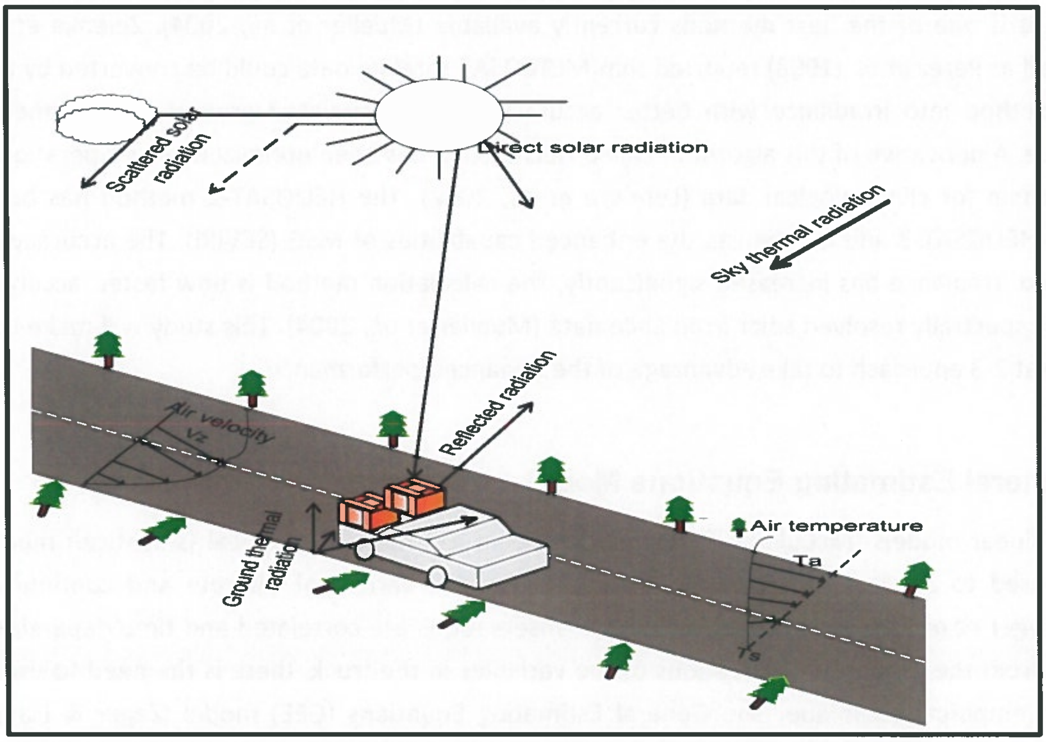

Figure 2-2 Energy exchanges for trucks loaded with Tomatoes. Modified from Porter *et al.* (1973)

From Figure 2-2, a truck loaded with tomato crates is subjected to three main sources of radiation. These are direct solar radiation, sky thermal radiation and radiation scattered by clouds and other atmospheric particles. Part of this energy is reflected by the tomatoes whilst part is absorbed. The amount of energy absorbed coupled with the ground thermal radiation cause the in-cargo micro-climate to fluctuate leading to heat build-up. The air stirred by the speeding trucks then moves swiftly over the produce which also affects the in-cargo micro-climate.

2.8. The Integrated Data Viewer (IDV)

The integrated Data Viewer (IDV) was conceptualized at the Unidata Program Center (UPC), part of the University Corporation for Atmospheric Research, Boulder, Colorado. The IDV brings together the capability to display and work with satellite imagery, gridded data and surface, upper air, and radar data within a unified interface. It also allows for the computation and display of built-in and user-supplied formula-based derived quantities (Murray *et al.*, 2003). The IDV release includes a Java™-based software library, and applications made from that software.

2.9. Firmness Decay of Tomatoes

According to Van Dijk & Tijskens (2000), the texture and firmness of fruits and vegetables depend on the presence and interactions of different chemical components, such as pectins in the middle lamellae and cellulose/hemi-cellulose matrix in the primary cell wall, as well as on physical aspects like archestructure and turgor. During transportation and storage some of these chemical components or physical aspects are affected, whilst others are not. Therefore it is assumed that the firmness of fruits and vegetables consists of two parts, a variable part and a fixed part. Components adding to the fixed part of the firmness include the (chemically inert) cellulose/hemi-cellulose matrix. Turgor and part of pectin that is susceptible to enzymatic degradation constitute the variable part of the firmness. At constant external conditions (like temperature in the climate controlled chamber) an analytical solution can be obtained for both firmness aspects by solving a set of analytical equations (Van Dijk *et al.*, 2006).

2.10. Mapping and Modelling Firmness Loss of Tomatoes

One significant factor that affects the marketable value of crops is quality information, but it has not received enough attention as compared to yield (Qiao *et al.*, 2005). It has however, not been established by earlier studies that firmness loss of tomatoes during dynamic condition in transport can be mapped. Qiao *et al.* (2005) argues that the absence of quality map studies could be due to the fact that quality information has more parameters than yield.

Van Dijk *et al.* (2006) further contended that quality evolution experiments are normally conducted at constant external conditions for example, temperature. To analyse the experimental data, analytical solutions of the model formulation at constant external conditions are therefore required. These analytical solutions are deduced from the analytical equations; however they are only applicable at constant conditions. In reality, constant conditions are rare. The model formulations applicable at any time and temperature are the analytical equations. The development of the analytical equations is the nucleus of the model rather than the ensuing analytical solutions. These analytical solutions are a logical outcome of the analytical equations.

3. Research Methods

3.1. Study Route

The study was conducted on the principal tomato trade route between Burkina Faso and Ghana (Figure 3-1). This study however, restricts itself to the Ghana part of the Burkina Faso –Ghana transportation corridor. A buffer of 30Km distance was created around this road network for the retrieval of the remote sensing imagery. This buffer distance represents 10 pixels of the METEOSAT images. The entire research design has been diagrammatically presented in Figure 1-2 above.

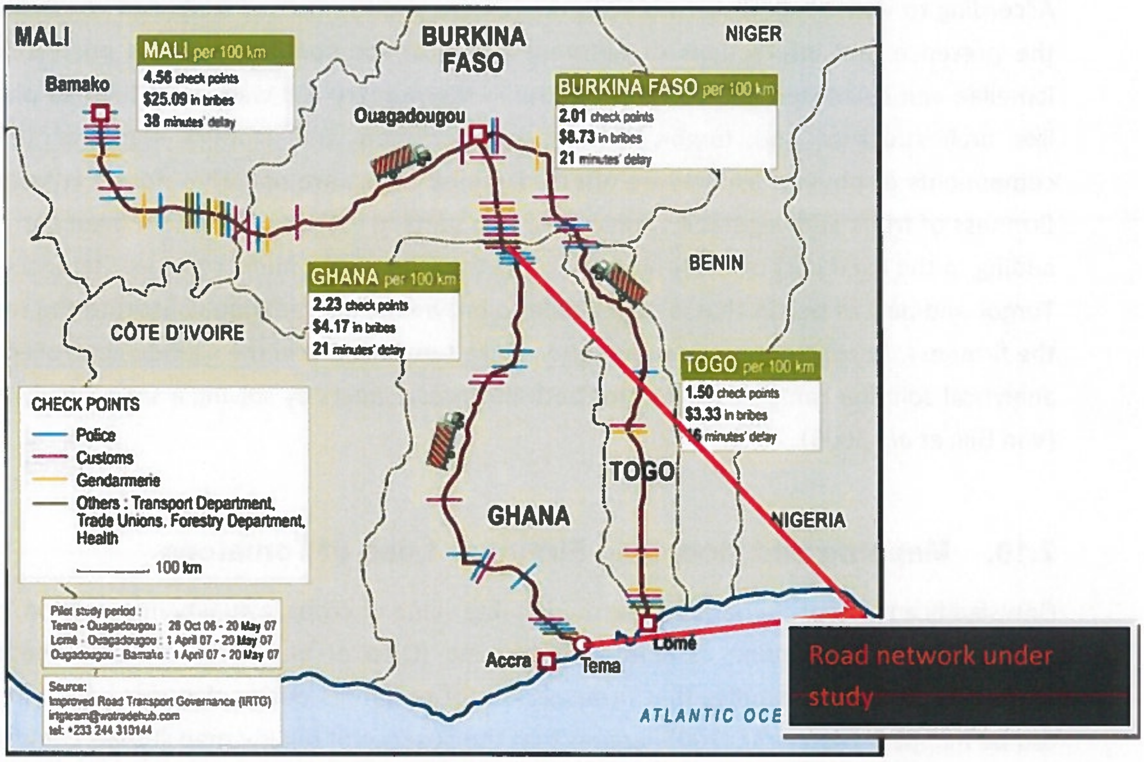

Figure 3-1 Map of the study route: Source (USAID, 2008).

3.2. Remote Sensing Data

A multi-temporal data of 15 minutes resolution was obtained from METEOSAT satellite. This was used to estimate the land surface temperature and solar radiation along the road corridor. This data was delivered by EUMETSAT through the remote server at ITC. These near real time imagery were chosen in such a time that it coincided with the period when the in-cargo micro-climate and other field data were collected.

3.3. Field Work

The field work was conducted by first doing situational analyses to assess the nature of tomato transportation within the study area. A number of organizations and individuals were consulted. Notably among them are the Ghana's Ministry of Food and Agriculture (MOFA) and Tomato Traders and Transporters Association of Ghana. This baseline study revealed that tomato movement within the West African sub-region is purely a seasonal activity. At the time of this survey, tomatoes were being moved from Ghana to Niger through Burkina Faso and Mali. The second phase of the field work involved the real problem of joining the transporters. The starting point for the field work was Tuobodom, a major tomato growing town in the Brong Ahafo region in the middle of Ghana. Data were collected on the following:

3.3.1. Determination of System Boundary for In-cargo Micro-climate

This was done by placing a temperature sensor on top of the upper layer of the tomato crates (i.e. Line AB in appendix 7.1) Data obtained from this sensor was then compared with data obtained from another sensor used to collect data on the outside air temperature. Then, the system boundary was finally assumed as the truck consisting of one big volume of water and that sampling done at any part will represent the entire phenomena except of course, at the extremities, which were avoided because of edge effects.

3.3.2. In-cargo Micro-climate and Outside Conditions Data

A HOBO weather station containing sensors for temperature, RH, wind speed, Photosynthetic Active Radiation (PAR) and light intensity were used. Some of the sensors were placed inside the tomato crates whilst some were positioned to collect data on outside environmental conditions. At the middle of the truck was a metallic pole to which the sensors for the outside environmental variables were mounted. The sensor for outside air temperature and relative humidity was enclosed in a radiation shield so as to guard against external factors. All The in-situ measurements were recorded every minute by the programmed weather sensors and then stored in a data logger. Data from identical sensors at different positions were averaged to give a single value per every logging interval. Subsequently, all per minute measurements for both in-cargo micro-climate and outside conditions were integrated to a 15 minute average readings to coincide with the satellite overpass time.

Tomato skin temperature was measured by a HOBO U12-006 4 channel extensions. Each of the extensions was placed at a corner of the tomato crate. With a logging interval of 1 minute, the values were aggregated to give an average per minute tomato skin temperature along the transportation corridor. A mercury thermometer was used to calibrate this 4 channel sensor. The calibration was done by placing both the mercury thermometer and the sensor in water with an initial temperature of 50^{oC}. The water was increasingly cooled by adding ice. The temperature values at every 30 seconds were recorded and then plotted. The polynomial equation with the highest R^2 was then used to calibrate the values obtained from the 4-channel sensor. The accuracy of the sensors after calibration improved from $\pm0.65^0$C to $\pm0.11^0$C.

Figure 3-2 illustrates the position of the sensors in one of the trucks. The lateral view of the trucks showed that there are 9 columns (1, 2 ....9) and 4 rows (i ...iv) of tomato crates loaded into the truck. Each column is made up of 3 layers (a, b and c) stacked on top of them. This results in 9 columns x 4 rows x 3 layers yielding a total of 108 tomato crates in the truck.

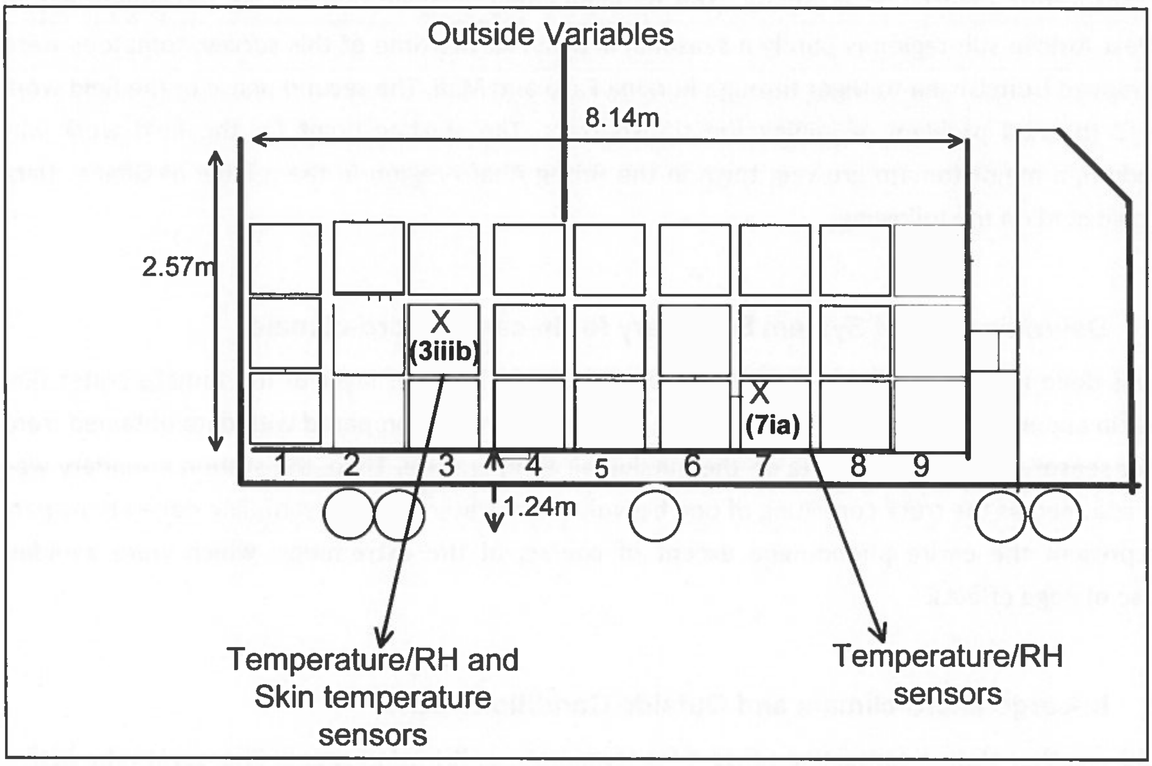

Figure 3-2 Lateral view of Tomato truck showing the location of sensors

3iiib indicates that the sensors for temperature, Relative humidity and the tomato skin temperature were placed in the 3rd column, 3rd row and in the second layer. The other sensor for temperature and relative humidity was also placed in 7th column, first row and then the first layer. The sensors for the outside variables were mounted on the pole in the middle of the truck as shown.

3.3.3. Tracklog

Per minute Track log of GPS points were also taken along the road with an HP iPAQ system (Figure 3-3). These were integrated with the temporal resolution of the SEVIRI sensor in order to correlate the remotely sensed environmental variables with the in-cargo micro-climate. In addition, the duration of the transport at every GPS location were recorded. The iPAQ was placed in another vehicle which closely followed the truck. This was however, done for only the first trip. For the subsequent trips, the iPAQ was placed inside the truck itself in such a way that the signals from the satellite were not interrupted. Also, the dimensions of the trucks including the length, width, height and ground distances were measured by a tape and then recorded.

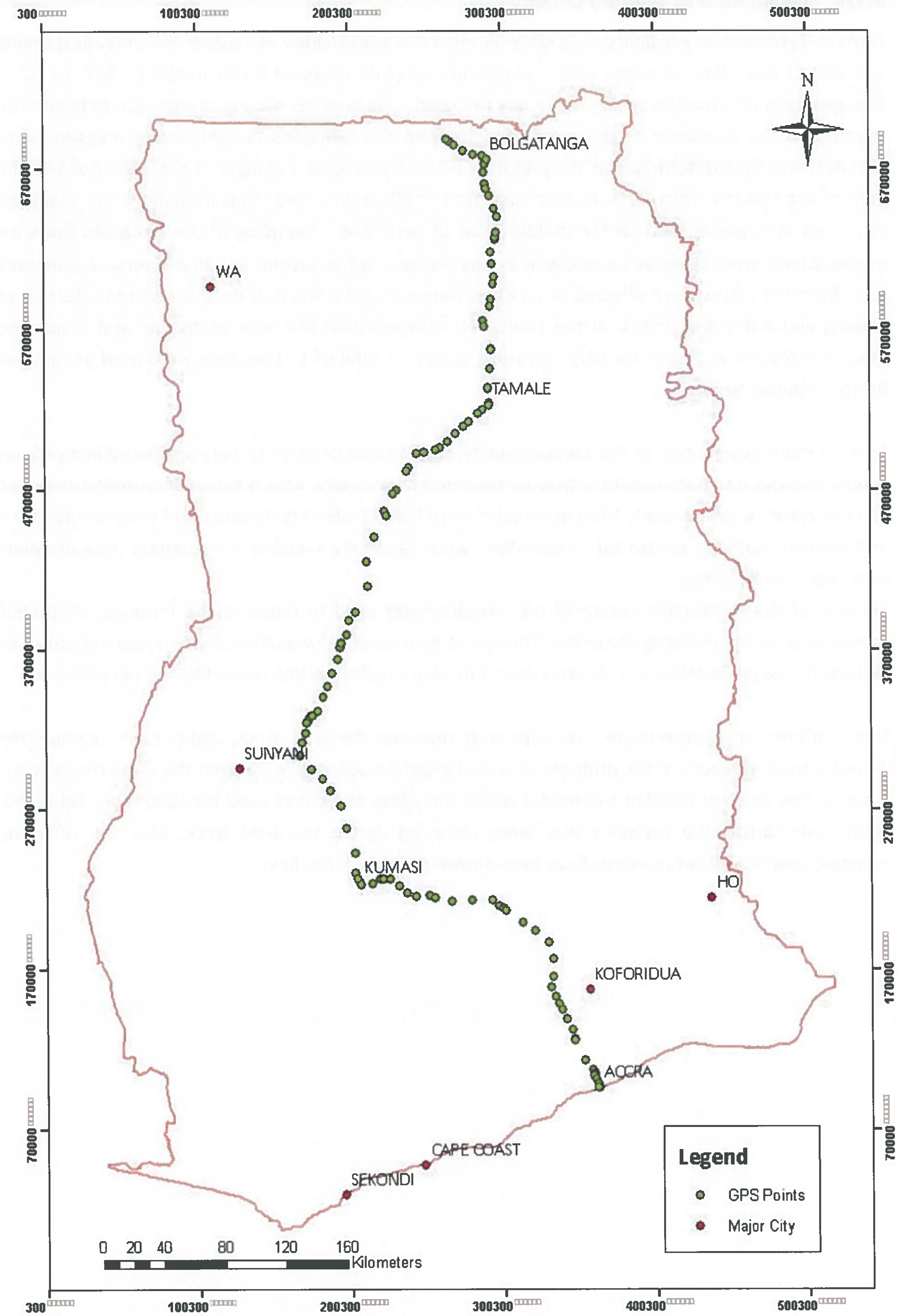

Figure 3-3 Point map of GPS Tracklogs for each minute during travel

3.3.4. Evaluation of Tomato Quality

Tomato (*Lycopersicon esculentum*), quality (Firmness) was evaluated at loading and offloading points and also at few other locations with a penetrometer (fruit pressure tester model FT 327 3-27Lbs). The approach of Schouten *et al.* (2007) was followed. This involves placing the tomato between the thumb and the forefinger of the right hand to keep the tomatoes upright during measurement. Firmness was then determined as the pressure necessary to force a plunger of specified size into the pulp of the tomato. This pressure was measured in Kilograms. Two measurements were made on each fruit at opposite ends, at the middle point of each side. Sampling of the tomatoes fruits for measurement were done by randomly selecting 4 crates in the second and first layers. 3 tomatoes each from the crates were selected at random. However, we could only do this random selection at loading and offloading points. In the course of transportation this was impossible and hence the random selection was done for only accessible crates. A total of 12 tomatoes were used as samples for the firmness tests.

To have more observation of the tomato quality, the in-truck conditions were simulated in a pick-up vehicle and more tomato quality data were recorded periodically. Also, a climate controlled chamber in a laboratory was also used. Tomato samples were loaded into this chamber and then temperature and relative humidity controlled. 5 tomatoes were randomly selected for firmness measurement every hour within a day.

Because of the destructive nature of the penetrometer used to measure the firmness, evaluated tomatoes were immediately discarded. The use of new tomato for each evaluation was necessary to exclude the negative effect of manual contact and also the destruction caused by the penetrometer.

Three different trips were made. Two trips were made on the same truck, and one on a completely different truck. Because of the principle of cross validation adopted, data from the same trucks were more or less used to develop the model whilst the other truck was used for validation. Table 3-1 below summarizes the variables that were recorded during the field work. Also the software packages used for all data analysis have been shown in Table 3-2 below.

Variable	Unit of Measure	Source		Estimated Variables	Instrument/ Technique	Application
		Field data	Download/ Meteosat			
Brightness temperature			X		SEVIRI	LST
Emissivity			x		SEVIRI	LST
Cloud index	Radians			X	SEVIRI	LST
Cloud mask				X	SEVIRI	LST
Zenith angle				X	SEVIRI	Radiation/LST
Air mass				X		Radiation
Rayleigh Optical				X		Radiation
Link Turbidity				X		
Temperature	^0C	X				In-cargo micro-climate models/Quality model
Relative humidity	%	X				
Light intensity	*Lux*	X				
Wind speed	Ms^{-1}	X				In-cargo micro-climate models
PAR	*μe*	X				
Surface area	m^2	X				
Truck dimensions	*m*	X				
Tomato skin temperature	^0C	X				
Time after harvest	*Hours*	X				
Tomato firmness[1]	*Kg*	X				Quality model

Table 3-1 Summary of variables recorded during field work

The shaded regions are those variables directly collected during the field work. The others were derived from IDV processing of the remote sensing imagery

[1] Variables collected to model the tomato firmness include, temperature (^0C), light intensity (Lux), RH (%) and time after harvest (hrs). These were collected mostly in climate controlled chamber and simulated conditions in pick-up truck.

Software	Application
IDV	Estimation of LST and radiation
ArcGIS 9.2	Mapping in-cargo micro-climate and quality loss
SPSS 16.0	Fitting GEE models and other statistical analysis
Maple 10.0	Analytical equations for firmness loss
MS. Excel	Parameter optimization problem, general data analysis and presentation
Math Type 6	Equations editor

Table 3-2 Software packages used in the study

3.4. Data Analysis

The data were analysed using 3 main techniques [i] Remote sensing algorithms comprising of the 4 channel Split Window algorithm for LST estimation and Heliosat-2/3 method for the estimation of solar radiation in IDV. [ii] The General Estimating Equations (GEE) Model for in-cargo relative humidity. [iii] A non-linear optimization and analytical approach to estimate quality losses and finally mapping quality loss in a GIS environment.

3.4.1. Estimation of land Surface Temperature from METEOSAT /8 SEVIRI

Land surface temperature (LST) for points along the road network were estimated by the four channel ($T_{3.9}$, $T_{8.7}$, $T_{10.8}$, T_{12}) split window algorithm. The 4 channel split window algorithm (Sun & Pinker, 2007) is given as:

$$T_s(I) = a_0(I) + a_1(I)T_{10.8} + a_2(I)(T_{10.8} - T_{12.0}) + a_3(I)(T_{3.9} - T_{8.7}) + a_4(I)(T_{10.8} - T_{12.0})^2 + a_5(I)(\sec\theta - 1) + a_6(I)T_{3.9}\cos\theta_s$$

Equation 1 Four-channel Split Window Algorithm

Where

I = the surface type index,

a_i = are the regression coefficients dependent on surface types.

Θ = Satellite Zenith angle

θ_s = Solar Zenith angle

The algorithm above includes a correction for atmospheric effects. The mid infrared channel, $T_{3.9}$ has low atmospheric absorption and attenuation and hence can be used to improve atmospheric correction after accounting for solar signals during the day time.

The emissivity effects are now considered through the surface type. Sun and Pinker (2003) demonstrated that using land cover types instead of the traditional surface emissivity helps to reduce the LST retrieval errors. The land cover types will be obtained from the 1km resolution land cover map maintained by the University of Maryland, department of Geography at the website http://glcf.umiacs.umd.edu/data/landcover.

In retrieving land surface temperature (LST) from MSG SEVIRI thermal bands, it is important not to mix the LST with cloud top temperature. Thus LST should be estimated under clear sky conditions. Following the approach of Cumba (2006), the clouded pixels were skipped by applying the cloud mask. The procedure detects clouded pixels using a threshold value specifically formulated for MSG. Satellite and solar Zenith angles were determined by satellite and sun triangulations implemented in the Abstract Data Distribution Environment (ADDE) server at ITC.

3.4.2. Estimation of Solar Radiation from Meteosat /8 SEVIRI

The general idea of the HELIOSAT method for the estimation of surface solar irradiance from satellite images is to deal with atmospheric and cloud extinction separately. In a first step the clear sky irradiance for a given location and time is calculated. In a second step, a cloud index is derived from METEOSAT imagery to take into account the cloud extinction. This step uses the fact that the reflected radiance measured by the satellite is approximately proportional to the amount of cloudiness characterized by the cloud index. This value then is correlated to the cloud transmission. Finally, the clear sky irradiance is reduced due to the cloud transmission to infer the surface irradiance.

Clear Sky Radiation

For the calculation of the clear sky irradiance, a direct irradiance model (Page, 1996) and a diffuse irradiance model (Dumortier, 1995) cited in Hammer *et al.* (2003) were applied. These models were developed by an empirical analysis of ground data and use the Linke turbidity factor to describe the atmospheric extinction. The direct normal irradiance G_{dn} is then given by:

$$G_{dn,clear} = G_{sc} \varepsilon e^{-0.8662 . TL(2) \delta R(m) m}$$

Equation 2 Direct normal irradiance

Where

$G_{dn,clear}$ = the clear sky direct irradiance

G_{sc} =the solar constant,

ε = the eccentricity correction,

TL (2) = the Linke turbidiy factor for air mass 2,

$\delta_R(m)$ = the Rayleigh optical thickness

m = the air mass and

e = Mathematical constant.

Linke Turbidity is explained as the number of Rayleigh atmospheres necessary to represent the actual thickness. The eccentricity correction, ε is given by:

$$\varepsilon = 1.000110 + 0.034221 \cos\Gamma + 0.001280 \sin\Gamma + 0.000719 \cos 2\Gamma + 0.000077 \sin 2\Gamma$$

Equation 3 the eccentricity correction

The clear sky diffuse radiation is also give by

$$G_{dif,\,clear} = G_{ext}\varepsilon\,(0.0065 + (-0.045 + 0.0646T_L\,(2))\cos\theta_z + (0.014 - 0.0327T_L\,(2))\cos 2\theta z)$$

Equation 4 Clear sky diffuse radiation

Where
$G_{dif,\,clear}$ = clear sky diffuse radiation and
G_{ext} = the extraterrestrial radiation.
Θ_z = Zolar zenith angle in degress

The final total clear sky radiation is the sum of clear sky diffuse radiation and clear sky direct irradiance expressed as:

$$C_{lear} = G_{dn,\,clear}\cos\theta_z + G_{dif,\,clear}$$

Equation 5 Total clear sky radiation

Cloud Transmission

Clouds have the largest influence on atmospheric radiation transfer. The cloud amount is derived from METEOSAT imagery. First the METEOSAT images are normalized with respect to the solar zenith angle. Therefore a relative reflectance is introduced. The measured reflectance is usually low for earth surfaces and high for clouds. A measure of the cloud cover, a cloud index can the then be introduced. It varies between 0 for cloud free pixels and 1 for overcast conditions.

$$n = (þ - þ_{ground}) / (þ_{cloud} - þ_{ground})$$

Equation 6 the cloud index

Where þ = albedo and the ground reflectance ($þ_{ground}$) will be derived from

$$þ_{ground} = þ_0 * þ_{shape}$$

Equation 7 Ground reflectance

$þ_0$ is a constant reflectivity value and $þ_{shape}$ is the ground shape function

The ground shape function is obtained by plotting one month time series of surface reflectivity against the co-scattering angle which is the angle between the direction of the sun and satellite as seen from the ground. This monthly calculation is done to account for seasonal variations of the ground reflectance.

Cloud transmission can then be described by the clear sky index kT* which normalizes the actual surface irradiance G with the clear sky irradiance G_{clear} from Eq. (5) as:

$$K_T^* = \frac{G}{G_{clear}}$$

Equation 8 Clear sky index

Finally the total surface irradiance is obtained from eqs [5] and [8] and computed as:

$$G = k_T*(G_{dn,\ clearcos\theta 2} + G_{dif,}$$

Equation 9 Total surface irradiance

Note that clear sky direct irradiance, $G_{dn,clear}$ and clear sky diffuse radiation, $G_{dif,clear}$ are obtained from eqs [2] and [4] respectively. For detail description of the HELIOSAT-3 method, see (Hammer *et al.*, 2003). A general overview of the HELIOSAT method is presented in Figure 3-4 below.

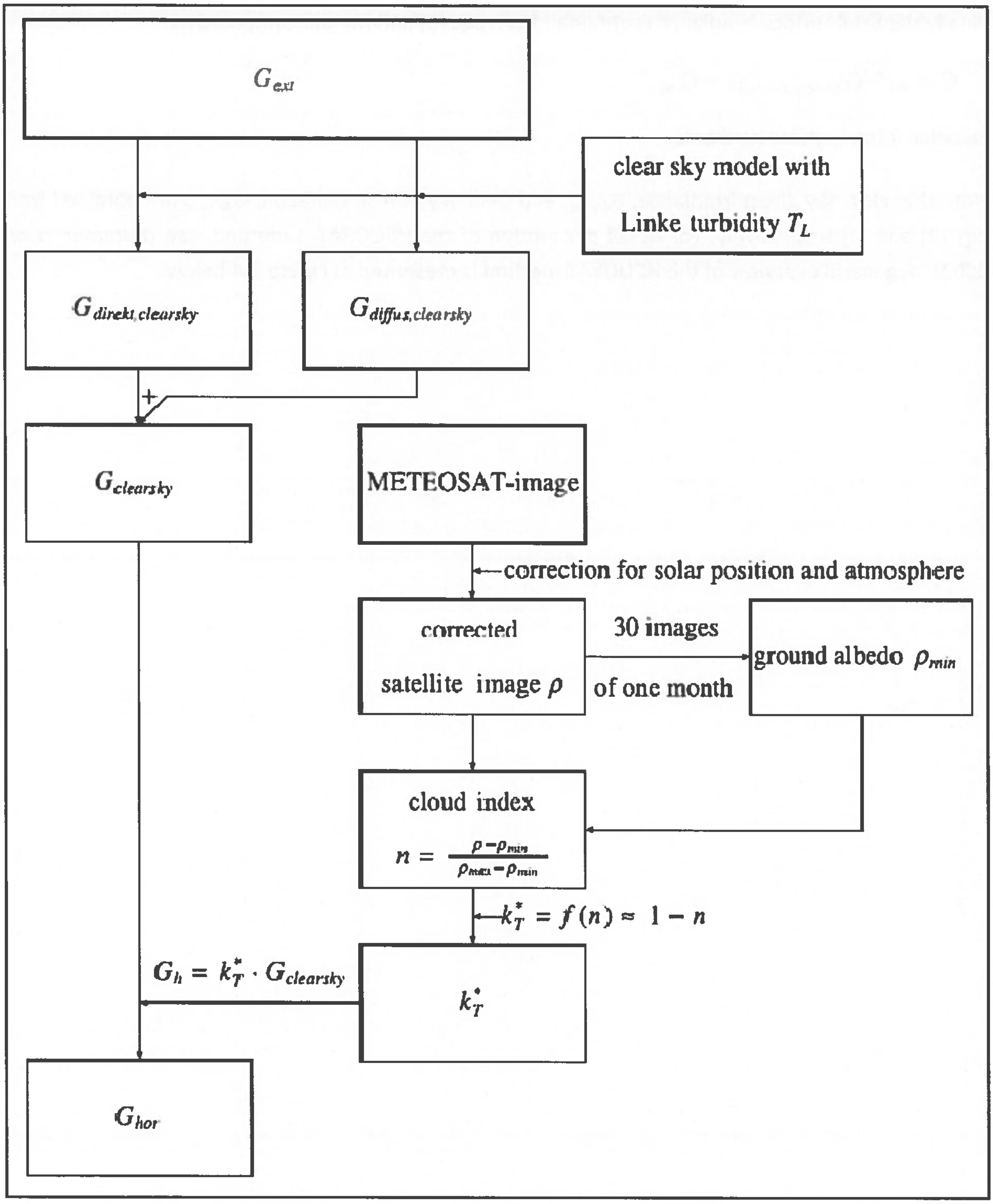

Figure 3-4 Overview of the HELIOSAT method: Source (Hammer *et al.*, 2003)

3.4.3. General Estimating Equations Model

The GEE is an extension of the quasi-likelihood approach (Zeger & Liang, 1986) and it is widely used to analyse longitudinal and correlated data (Hanley *et al.*, 2003). Longitudinal data sets encompass repeated observations of an outcome variable and a set of covariates or explanatory variables (Zeger & Liang, 1986). This method allows for a correlation structure for longitudinal (one-dimensional, e.g., time series) data analysis. This special data layout is required when responses are measured continually on the same subject or unit across time. Therefore, the GEE method takes into account correlations within these units, while correlations between units can be assumed to be zero (Carl & Kühn, 2007).

In this context, GEE is the most appropriate statically model because of the following reasons [i] since the measurements of the outcome variables (micro-climate) inside the trucks are repeated measurements on the same subject, correlation is expected [ii] This correlation may be a function of time [iii] Observations in different trucks are independent of one another [iii] the average response of the observations from different trucks (marginal expectation) share the same covariates of outside environmental conditions. For detail description of this model, see (Halekoh *et al.*, 2006; Liang & Zeger, 1986; Zeger & Liang, 1986).

3.4.3.1. Fitting the GEE Model

The basic assumption employed by GEE is that a known transformation of the marginal expectation of the response is a linear function of the covariates and that its variance is a known function of its expectation (Zeger & Liang, 1986). This known transformation of the response variable is called the mean link function and allows for the estimation of the model. To predict the in-cargo temperature, the distribution of this response variable was found to be normal and thus we made use of the Identity mean link function. The identity link function is given as $f(x) = x$. From this, the relationship between the in-cargo temperature and the covariates can be given as:

$$f\,(T_{incargo}) = T_{incargo} = f(LST + T_{air} + W_s)$$

Equation 10 GEE functional relationship of in-cargo temperature

$$T_{incargo} = b_0 + b_1 LST + b_2 T_{air} + b_3 W_s$$

Equation 11 GEE model of in-cargo temperature

Where, $T_{incargo}$ = in-cargo temperature (^{0}C), LST = land surface temperature (^{0}C), T_{air} = outside air temperature (^{0}C) and W_s = the speed of the wind blowing over the tomato crates (ms^{-1}), b_0 = the intercept, b_1, b_2 and b_3 are the regression coefficients of the covariates

Similarly, for both the in-cargo relative humidity and light intensity, the distributions were found to follow the Gamma curve and the log mean link function was adopted. The log link function is given as $f(x) = \log(x)$.

Thus,

$$f\,(RH_{incargo}) = \log(RH_{incargo}) = f(RH_{out} + T_{skin} + T_{air})$$

Equation 12 GEE functional relationship of in-cargo relative humidity

$$\text{Log}\,(RH_{incargo}) = b_0 + b_1RH_{out} + b_2T_{skin} + b_3T_{air}$$

Equation 13 GEE model for the in-cargo relative humidity

$$f(LI_{incargo}) = \log\,(LI_{incargo}) = f(R)$$

Equation 14 GEE functional relationship of in-cargo light intensity

$$\text{Log}\,(LI_{incargo}) = b_1R$$

Equation 15 GEE model of in-cargo light intensity

Where $RH_{incargo}$ = in-cargo relative humidity (%), RH_{out} = outside relative humidity (%), $LI_{incargo}$ = in-cargo light intensity (Lux) R = solar radiation (Wm^{-2}), T_{skin} = tomato skin temperature b_0 and b_1 are the regression parameters.

Consider a sample of i = 1. . . K independent multivariate observations Yi = (Yi1. . . Yit. . . Yini). Here i represent a truck with n_i observations. The expectations $E(Y_{it}) = \mu_{it}$ are related to the p dimensional regressor vector x_{it} by the mean-link function g

$$g(\mu_{it}) = \chi_{it}^T\beta$$

Equation 16 Mean link of the expectations

This implies that the GEE regression equation for the in-cargo micro-climate is given as:

$$E[Y_{it}] = \mu_{it} = \chi_{it}^T\beta$$

Equation 17 GEE regression equation for the in-cargo micro-climate

Where Y_{it} = is the marginal expectation (average response) of the dependant variable for truck, i at time, t and β consists of the regression coefficients.

Let

$$VAR(Y_{it}) = \phi a_{it}$$

Equation 18 Variance estimator

Where ø is a common scale parameter and ait = a(µit) is a known variance function. Let Ri(α) be a working correlation matrix completely described by the parameter vector α of Length, m.

Let

$$V_i = \phi A_i^{1/2} R_i(\alpha) A_i^{1/2}$$

Equation 19 Working correlation matrix of the expectations

Be the corresponding working covariance matrix of Yi, where Ai is the diagonal matrix with entries a_{it}. For given estimates ($\acute{\phi}$, $\acute{\alpha}$) of (ϕ, α) the estimate $\hat{\gamma}$ is the solution of the equation:

$$\sum_{i=1}^{k} \frac{\partial \mu_i^T}{\partial \beta} V_i^{-1} (Y_i - \mu_i) = 0$$

Equation 20 Parameter estimation of the working correlation matrix

Liang and Zeger (1986) suggest using consistent moment estimates for ϕ and α. This yield an iterative scheme which switches between estimating β for fixed values of $\acute{\phi}$ and $\acute{\alpha}$ and estimating (ϕ, α) for fixed values of $\hat{\gamma}$, this scheme yields a consistent estimate for β. Moreover, $K^{1/2}$ ($\hat{\gamma}$ - β) is asymptotically multivariate normally distributed with zero mean and covariance matrix:

$$\Sigma = \lim_{k \to \infty} K \Sigma_0^{-1} \Sigma_1 \Sigma_0^{-1}$$

Where

$$\Sigma_0 = \sum_{i=1}^{K} \frac{\partial \mu_i^T}{\partial \beta} V_i^{-1} \frac{\partial \mu_i}{\partial \beta^T}, \Sigma_1 = \sum_{i=1}^{k} \frac{\partial \mu_i^T}{\partial \beta} V_i^{-1} \mathrm{COV}(Y_i) V_i^{-1} \frac{\partial \mu_i}{\partial \beta^T}$$

Equation 21 Final parameter and working correlation matrix estimations of the GEE model

Replacing β, ϕ and α by consistent estimates and the covariance matrix COV(Yi) by (Yi – μi)(Yi–μi)> in [15] yields a so called sandwich estimate $\grave{E}$ of Σ. The estimate $\grave{E}$ is a consistent estimate of Σ even if the working correlation matrices Ri(α) are mis-specified.

For the in-cargo temperature, the exchangeable working correlation matrix was used based on parsimony and fit whilst the autoregressive, AR (1) was used for the in-cargo relative humidity and light intensity. The software package SPSS 16.0 was used to fit this model.

3.4.4. Validation of In-cargo Micro-Climate models

The K-fold cross validation was used to validate the in-cargo micro-climate models. This technique is used to validate statistical model by dividing the dataset into K subsets then leaves one out and trains the model with the rest of the dataset. The one that is left is used to validate the model. The process is then repeated K times so that all the subsets are used for validation once. This method was proposed by Verbyla & Litvaitis (1989) and adopted by Yáñez (2007). The data from the trucks were divided into two according to truck type and date of data collection. A small portion of the data from the 3rd truck was added to truck 2 data whilst the remaining data from 3 was combined with that of truck 1. Validation of the model predictions was tested by the coefficient of determination (R^2), student t-test and Root Mean Square Error (RMSE).

3.4.5. Development of Firmness Loss Model

The rate at which tomatoes soften during post-harvest depends on many factors. In this study, firmness loss of tomatoes after harvesting can be attributable to the micro-climate inside the trucks that transports the vegetables as well as the duration after harvest.

Mathematically, Firmness = f (temperature, light intensity, relative humidity, time). The decrease in firmness of tomatoes has been described extensively by Tijskens *et al.* (2002) and also Lana *et al.* (2005). In this study, a Maple software package (version 10.0) was used to solve the analytical equations (appendix 7.5) needed to describe the firmness loss of tomatoes during dynamic conditions in transport.

By applying existing mechanistic knowledge expressed in mathematical model, the firmness loss for constant conditions was derived as:

$$F(t) = F0\,\mathbf{e}\,(-RH0\;k\;L0\;t)$$

Equation 22 Firmness loss equation for constant conditions

Where

F (t) = Firmness at time, t (Kg) F0 = initial firmness (kg) RH0 = initial relative humidity (%)
k = rate constant of firmness decay (day^{-1}), L0 = initial light intensity (Lux), t= time period after harvest (hrs) and

Substituting RH0=aR + bR * RH and L0=aL + bL * L, this equation is obtained

$$F = F0*\exp(-(aR + bR*RH)*k*(aL + bL*L)*t)$$

Equation 23 Results of analytical equation of the firmness decay model

The rate constant of firmness decay, k depends on temperature according to Arrhenius law (Bastin & Dochain, 1990).

$$k = kref*\exp(120.2790474*Ea*(1 / Tref+273 - 1 / (T + 273)))$$

Equation 24 Arrhenius law

Where

Tref = reference temperature in ^{0}C assumed to be 20^{0}C
Kref = the rate, k at reference temperature ($hour^{-1}$)
Ea = energy of activation (kJ/mol)
RH = in-cargo relative humidity (%)
L = in-cargo light intensity (Lux)
t = time period after harvest (hours) and
T = in-cargo temperature (^{o}C)

aR, bR, aL and bL are the coefficients of the exponential relationship between firmness and relative humidity whilst aL and bL describe similar relations with the light intensity. The unknown parameters then become aR, bR, aL, bL, Ea, kref, the initital firmness, was measured immediately after harvesting the tomatoes was found to be 4Kg.

The Microsoft Office Excel Solver tool which uses the Generalized Reduced Gradient (GRG2) nonlinear optimization code was iteratively applied to obtain the model parameters in line with these steps:

1. Formulation of appropriate and realistic initial values. This was done by a critical look at the data and trial and error.
2. Estimate the unknown model parameters one at a time using the Solver functionality which finds the optimal value of the parameter.
3. Accept or reject the new model based on the trade-off between model structure and Absolute Total Errors (ABSe) between the measurements and the model outputs. The overall parameter estimation procedure is developed as non-linear optimisation problem which takes the form:

$$\min ABSe = \sum(y - \hat{y})$$

$$\hat{y}_{obs} = f(X, P)$$

Equation 25 Non-linear regression function for the firmness loss

Where, ABSe is absolute total error between the observed firmness and the model output, $\hat{y}_{obs}$ is observed firmness in Kg, X is a vector of model parameters and P is a vector of the explanatory variables.

4. Improving the model structure by varying the initial values and setting up upper limits based on:

- Mechanistic knowledge of the tomato quality evolution characteristics
- Observed correlation between data and model misfit.

5. After modifying the model structure, the modelling procedure then starts again from step 2.
6. The modelling procedure is terminated when optimal values have been found for each model parameter which minimise the absolute total error

The model output is then used to run a regression analysis with the observed firmness as the response variable and the model output as the predictor variable. The model output is then assumed to be linearly related to the observed firmness with zero intercept.

$$y = a.\,(X, P)$$

Equation 26 Final non-linear regression model for firmness loss

Where a = the regression coefficient.

3.4.6. Sensitivity analysis

A sensitivity analysis was done to test which in-cargo variable is more important in controlling the quality of the tomatoes. . A range of ±10% and ±30% was used for temperature, time and light intensity. Relative humidity was increased by 5% and then decreased by 30%. These explanatory variables were decoupled since they all affect tomato firmness and then studied independently to determine how each affected tomato quality during the dynamic condition in transport.

3.4.7. Mapping Quality Loss and In-cargo Micro-Climate

After the modelling procedure, quality represented by firmness was estimated for every 15 minutes interval during transportation and integrated with the tracklog data. Using the GIS-based regression procedure, maps of the observed in-cargo micro-climate together with the time period after harvest were created in a GIS environment (appendix 7.3). The Inverse Distance Weighted (IDW) interpolation scheme was used to create the raster layers including the quality maps. IDW interpolation explicitly implements the assumption that observations that are close to one another are more identical than those that are far away. To calculate a value for any unmeasured location, IDW will use the measured values adjoining the prediction location. The measured values closest to the prediction location will have more influence on the predicted value than the ones farther away. Accordingly, IDW assumes that each measured point has a local influence that diminishes with distance. It weights the points nearer to the prediction position greater than those far apart, hence the name inverse distance weighted (Chang, 2004). The diagram in Figure 3-5 summarizes the procedure followed in developing the quality and in-cargo micro-climate maps along the transportation corridor.

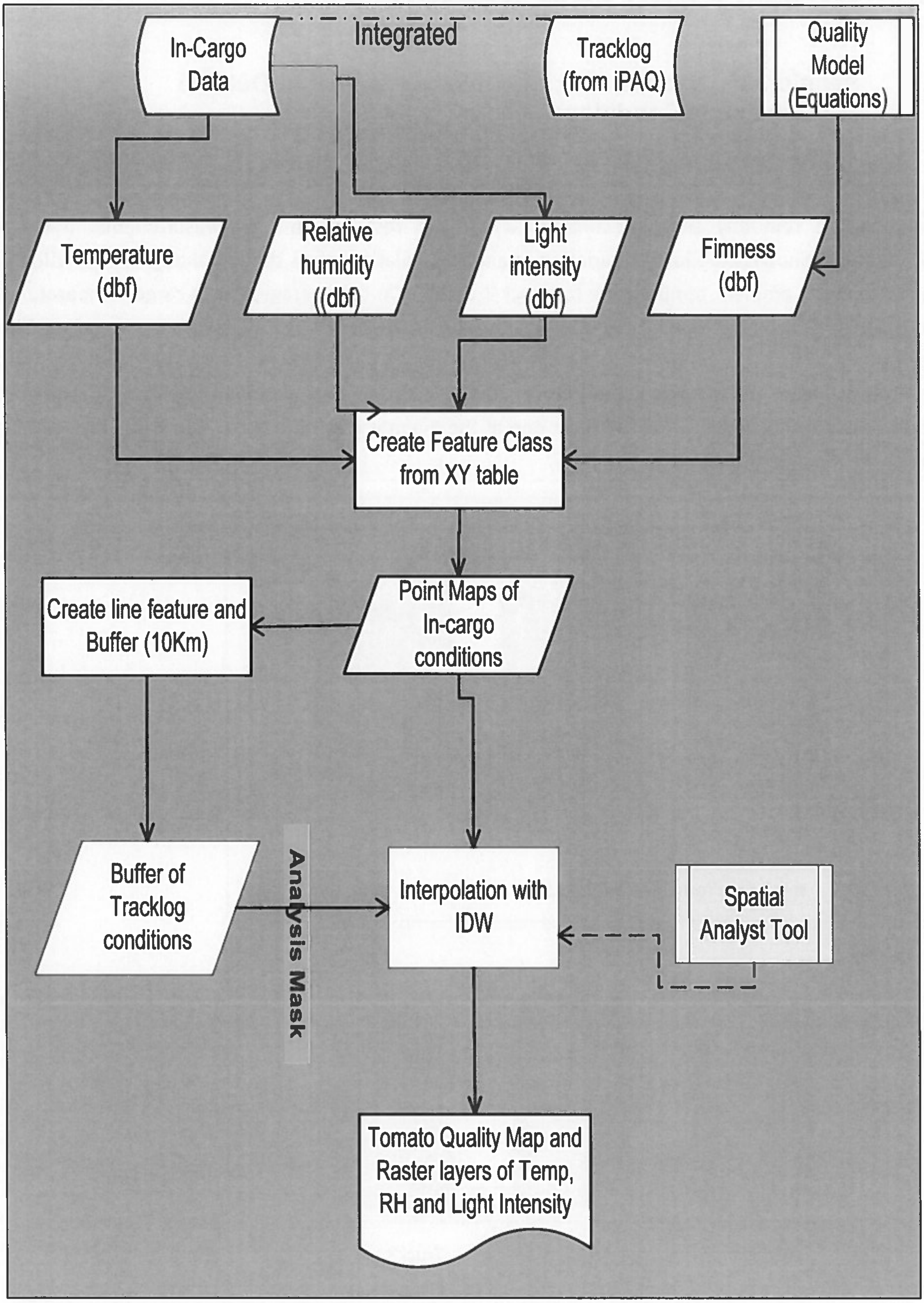

Figure 3-5 GIS-based regression mapping procedure

4. Results and Discussion

4.1. Relationship between In-cargo micro-climate and Outside Environmental Conditions

In Table 4-1 the descriptive statistics of the in-cargo micro-climate and the outside environmental conditions have been presented for the three trucks used in this study. The LST and the solar radiation are remotely sensed estimates whilst the rest are in-situ measurements. In-cargo temperatures showed the lowest variation (standard deviation) than the LST though its variation is higher than the ambient temperature for truck 1 and 3. On the average, the in-cargo temperatures were significantly higher than both the LST and air temperature throughout the transport period. The significance of this was confirmed using the Analysis of Variance (ANOVA) with the null hypothesis that the means of the in-cargo temperature, outside air temperature and the LST are the same as against the alternative which says at least one of the mean is different: Ho: $\mu_1 = \mu_2 = \mu_3$ Ha: At least one of the mean is different

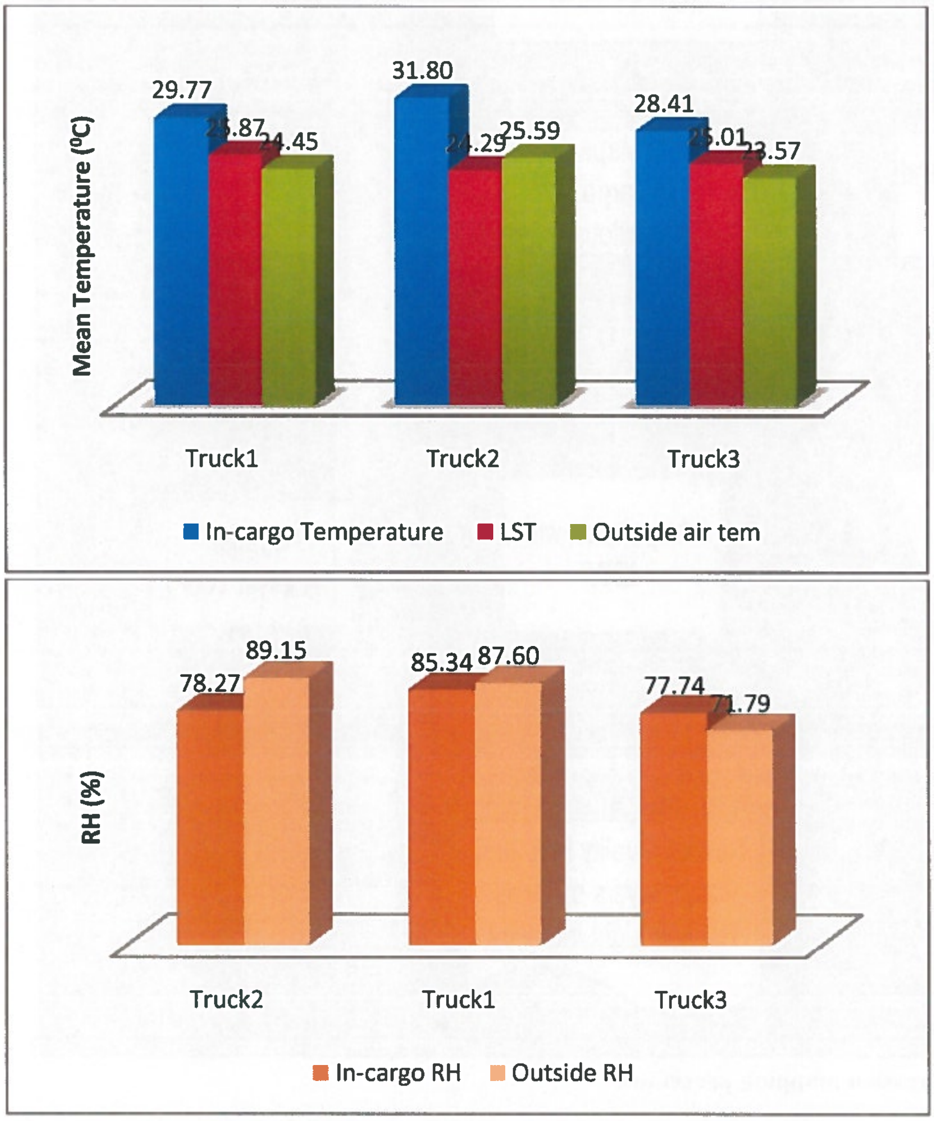

Figure 4-1 Comparison of different means [top] temperature [bottom] RH

From the ANOVA results, the null hypothesis that says that there is no difference between mean temperatures was rejected and conclusion that at least one of the mean temperature is significantly different was made (ANOVA, $F = 86.74$, df 2, 150, p-value < 0.000).

This result, shown graphically in Figure 4-1and Figure 4-2 is expected because the packaging of the tomato crates in the trucks leads to heat build up which cause the in-cargo temperature to rise above the outside air temperature and LST. Smargiassi *et al.* (2008) found similar results when he observed that indoor temperatures were generally higher than outdoor temperatures in a study involving 75 urban dwellings. The time plot in Figure 4-2 also shows that the in-cargo temperature falls below the LST and air temperature towards the end of the transport time which coincides with the early hours of the day. Both the LST and air temperature rises during the early hours because of increasing strength of incoming solar radiation. The in-cargo temperature does not respond quickly to changes in the LST and air temperature and shows a gradual decreasing trend.

In-cargo relative humidity values were lower than the outside relative humidity except for the 3rd

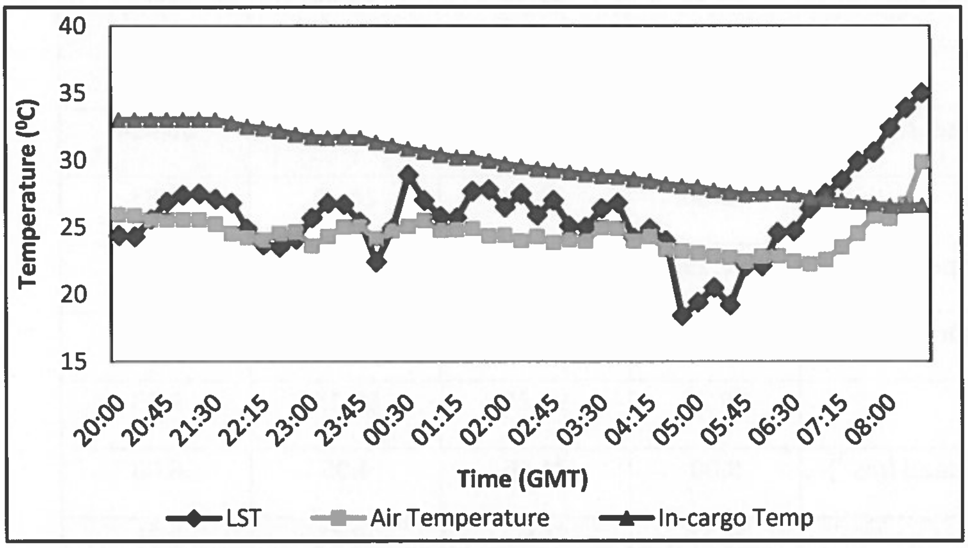

Figure 4-2 Time plot of air, in-cargo and Land surface temperatures

truck which we found a contrary phenomenon. A two sample t-test was used to asses whether this difference between the in-cargo RH and outside RH was significant. The null hypothesis formulated reads that the mean of the in-cargo RH is the same as the mean of the outside RH as against the alternative which says the two means are different (Ho: $\mu_1 = \mu_2$; Ha: $\mu_1 \neq \mu_2$). Assuming unequal variances, the null hypothesis was rejected and the conclusion was that the mean of the in-cargo RH is significantly different from the mean of the outside RH (2 Sample T-test, $t = 3.39$, df = 92.03, $P < 0.0001$)

Also, the in-cargo humidity values were less variable whilst the variability of the outside humidity values were more pronounced. This is probably due to the continued respiration activity of the fresh produce which seems to more or less regulate the amount of moisture within the tomato crates. This respiration activity releases moisture into the trucks which prevents excessive fluctuations of the in-cargo RH.

Truck ID	Variable	Minimum	Maximum	Mean	Standard deviation
1	Temperature (^{0}C)	26.57	33.01	29.77	2.21
	RH (%)	80.27	93.70	85.34	4.36
	Light Intensity (Lux)	0.00	1567.35	122.36	335.65
	LST (^{0}C)	18.40	35.00	25.87	3.21
	Air temperature (^{0}C)	22.25	29.85	24.45	1.31
	Radiation (Wm^{-2})	0.00	560.60	49.21	128.82
	RH (%)	55.05	95.25	87.60	7.70
	Wind Speed (ms^{-1})	0.00	9.11	4.54	3.09
2	Temperature (^{0}C)	28.75	35.95	31.80	2.30
	RH (%)	67.11	89.84	78.27	7.50
	Light Intensity (Lux)	0.00	1345.68	162.55	364.14
	LST (^{0}C)	13.80	44.90	24.29	5.83
	Air temperature (^{0}C)	22.19	34.66	25.59	3.17
	Radiation (Wm^{-2})	0.00	712.50	69.29	170.28
	RH (%)	69.23	97.25	89.15	9.33
	Wind Speed (ms^{-1})	0.00	34.56	4.05	6.08
3	Temperature (^{0}C)	23.69	34.08	28.41	3.33
	RH (%)	65.28	95.14	77.74	9.64
	Light Intensity (Lux)	0.00	2152.80	106.37	397.78
	LST (^{0}C)	15.60	37.50	25.01	4.23
	Air temperature (^{0}C)	20.39	28.31	23.57	2.25
	Radiation (Wm^{-2})	0.00	613.30	52.60	139.52
	RH (%)	38.00	88.92	71.79	11.30
	Wind Speed (ms^{-1})	0.00	2.49	0.87	0.79

Table 4-1 Summary descriptive statistics of the in-cargo and outside environmental conditions
Shaded regions are in-cargo variables and un-shaded regions are outside environmental variables

Figure 4-3A shows the relationship between the in-cargo temperature and LST. It is obvious that the relationship is non-linear. This was unexpected. A linear relationship has been anticipated between the two but it turned out that a polynomial of the 6th order best describes the relationship between the LST and in-cargo temperature. Transforming the in-cargo temperature values did not improve the linearity of the relation. The LST is however, strongly correlated with the air temperature (r = 70%).

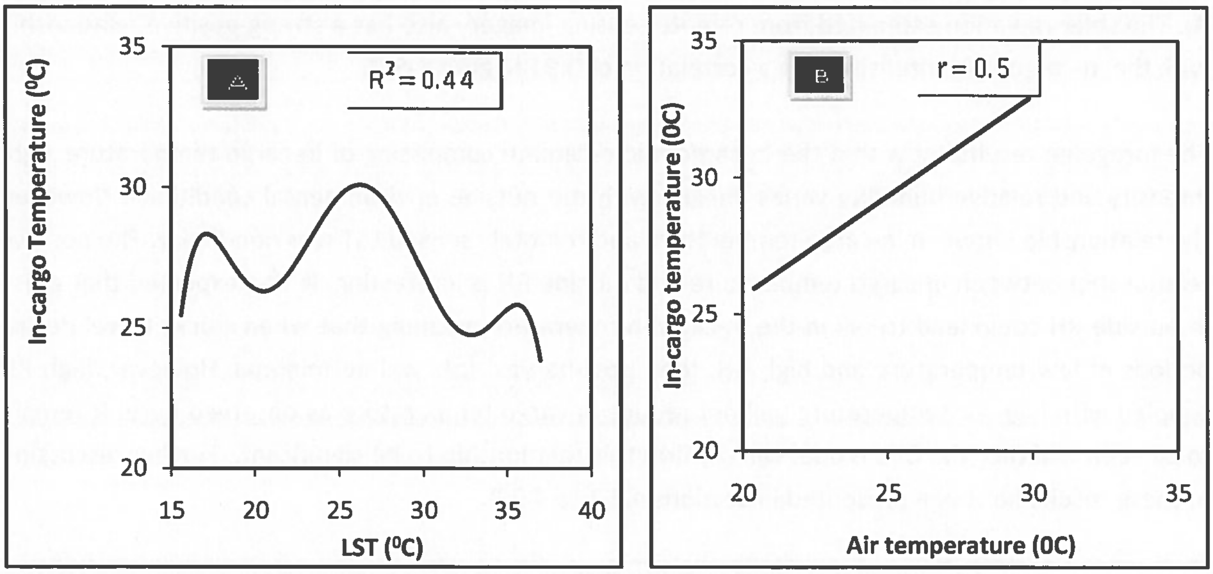

Figure 4-3 Relationship between in-cargo temperature and [a] LST, [b] air temperature

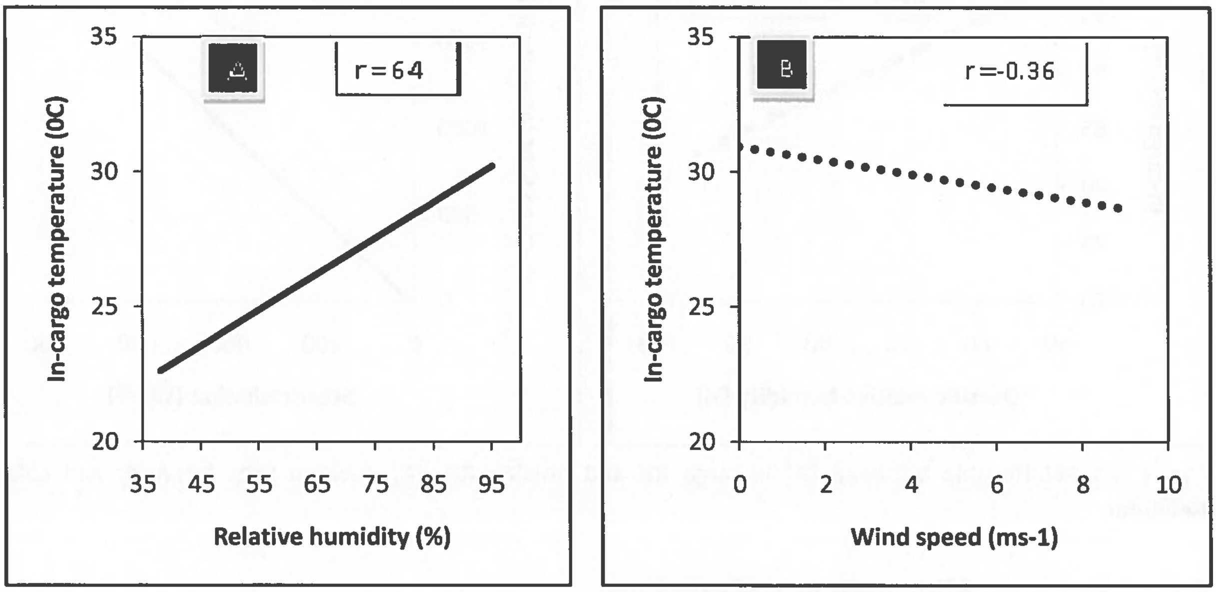

Figure 4-4 Relationship between in-cargo temperature and [a] relative humidity [b] wind speed

On the other hand, Figure 4-3 B illustrates the linear relationship between in-cargo temperature and the outside air temperature. The in-cargo temperature is positively associated with the air temperature with a correlation of 0.5.

Interestingly, there is rather a linear relationship between outside RH and in-cargo temperature (Figure 4-4 A). There is a strong positive association between the in-cargo temperature and outside RH with a correlation of 64%. There is also a negative linear relationship between the wind speed and that of the in-cargo temperature. The strength of this relationship is moderate(r=-0.36, Figure 4-4B).

The in-cargo RH has a negative association with the outside RH with a correlation of -0.57 (Figure 4-5 A). The solar radiation estimated from remote sensing imagery also has a strong positive relationship with the in-cargo light intensity with a correlation of 0.91 (Figure 4-5B).

The foregoing results show that the in-cargo micro-climate comprising of in-cargo temperature, light intensity and relative humidity varies linearly with the outside environmental conditions. However, the relationship between in-cargo temperature and remotely sensed LST was non-linear. The positive relationship between in-cargo temperature and outside RH is interesting. It was expected that a rise in outside RH could lead to fall in the in-cargo temperature meaning that when trucks travel during periods of low temperature and high RH, then post-harvest loss will be minimal. However, high RH coupled with high air temperature will not reduce in-cargo temperature as observed here. It remain to be seen whether the GEE model will confirm this relationship to be significant. Further discussion of these results has been presented in sections 4.2.1 to 4.2.3.

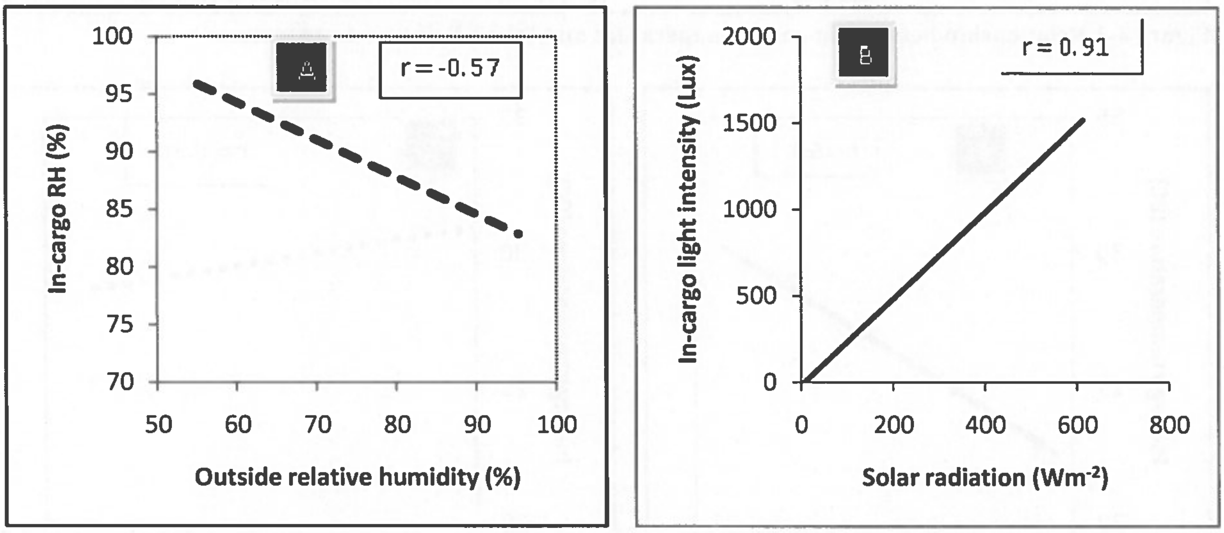

Figure 4-5 Relationship between [A] in-cargo RH and outside RH, [B] in-cargo light intensity and solar radiation

4.2. In-cargo Micro-climate Modelling

To model the in-cargo micro-climate of temperature, relative humidity and light intensity, use was made of the General Estimating Equations (GEE) Model. To avoid complexity in parameter estimation, the micro-climate was decoupled. Thus separate estimation procedures were done for each of the variables of in cargo micro-climate including temperature, RH and light intensity.

4.2.1. In-Cargo Temperature Prediction

Table 4-2 presents the GEE model prediction of the in-cargo temperatures. Because of the non-linearity relation between the in-cargo temperatures and LST, the later was excluded in the GEE model because it violates the fundamental assumption underlying the GEE model. Every 1^0C increment in air temperature is associated with 0.42^0C increase in in-cargo temperature. Also a 1% increase in the outside relative humidity led to an increase of 0.04^0C rise in in-cargo temperature whilst a unit rise in the speed of wind is associated with a 0.17^0C fall in in-cargo temperature. The GEE model explained 77% of the variability of the in-cargo temperatures. Using only the air temperature, 25% of the in-cargo temperature variance was explained (Figure 4-3B) whilst outside RH alone explained 41% of the variance (Figure 4-4A). From equation [11], the final predictor equation for the in-cargo temperature is given as:

$$T_{incargo} = 17.72 + 0.04RH_{out} + 0.42T_{air} - 0.17W_s$$

Equation 27 Final predictor equation for the in-cargo temperature

The slopes of all the predictor variables were significant ($P < 0.001$). This means that all the parameters were significantly different from zero and that a relationship exists between the in-cargo temperature and the predictors. Table 4-2 also shows that the estimated parameters have lower standard errors and the confidence intervals are within reasonable limits.

Validation

The validity of this model was tested using the RMSE, student t-test and R^2. The validation procedure followed the K-fold cross validation where the data from the three trucks were divided into two.
The averages of the R^2 and RMSE of the 'backward and forward' validations were found to be respectively 77% and 4.18^0C. The student t-test was also used to assess whether the model produces bias predictions. To do this, two null hypotheses were formulated.

H_o: intercept = 0 and H_o: slope $\beta_1 = \beta_2 = \beta_3 = 1$. The alternate hypothesis is:
H_a: intercept ≠ 0 and Ha: slope $\beta_1 \neq \beta_2 \neq \beta_3 \neq 1$

For the model to be free from systematic error or bias, these null hypotheses must hold. The alternative hypotheses, Ha says that the intercept is significantly different from zero and the slopes for all the explanatory variables are not equal to 1. These null hypotheses will be rejected if the test statistic, t is above the expected t value at $\alpha = 0.05$.
The student t-test, t is given as:

$$t = \chi - \mu o/se$$

Equation 28 the Student t-test for validation

Where χ is the coefficient (intercept b_0 or slopes b_1, b_2 and b_3) estimated by the model and μ_0 is the coefficient expected under the null hypotheses and se is the standard error of the estimates

Since the t- calculated are less than t-observed at 5% significance level, the test results showed that the model did not produce bias predictions and is free from systematic error or bias. We therefore failed to reject both null hypotheses and concluded that the model can be used to predict in-cargo temperature (Student T-test, T Slopes = -24.8, -270.6, -111.9, T intercept = -18.86, df = 86, α = 5% t* = 1.66).

	Estimate[2]	Standard error	95% Confidence interval	
			Lower	Upper
Air temperature	0.42	0.02	0.37	0.47
Outside relative humidity	0.04	0.006	0.02	0.05
Wind speed	-0.17	0.02	-0.21	-0.12
Constant	17.72	0.98	15.81	19.64
R-Square[3]	0.77			
RMSE	4.18			

Table 4-2 Parameter estimates of in-cargo temperature prediction

In this study, a GEE model was developed to predict the in-cargo temperature in the trucks used to transport tomatoes for every 15 minutes between October and November 2008 in Ghana. The model explains 77% of the variability in the in-cargo temperature. Studies that have reported on the relationship between indoor and outdoor temperatures observed that indoor and outdoor temperatures were linearly related especially in naturally ventilated enclosures (Smargiassi *et al.*, 2008). In this study also, both the in-cargo and outside air temperature vary together and further to that, the outside RH also varies linearly with the in-cargo temperature. These findings are quite interesting for managers in the horticultural supply chain desiring to control the temperature in the trucks used to transport fruits and vegetables in the region. Whilst it is impractical to control the outside RH and air temperature, understanding of the behaviour of the in-cargo temperature will improve the design of any cooling system. The negative relationship between wind speed and in-cargo temperature means that if road conditions are improved and truck drivers can drive a little faster within reasonable limits, in-cargo temperature can be reduced and this can lead to a reduction in firmness loss.

Smargiassi *et al.* (2008) also found a linear relation between surface and indoor temperatures when they placed 75 dwellings on a thermal map. However, this analysis found a rather non-linear relationship between in-cargo and surface temperatures. This is because the dynamics are entirely different for the two studies. In the case of Smargiassi *et al.* (2008), surface temperature may vary linearly with indoor temperature because the buildings are stationery and are in prolonged contact with LST over long periods. This can not be said of tomato trucks in constant motion and as such the

[2] All parameters were significant with $P < 0.001$

[3] Ratio of variance of predicted values to variance of observed values.

LST do not have direct effect on the temperature inside the trucks. The estimation of LST from MSG images thus did not provide much gain in explaining the variability of the in-cargo temperature because of the absence of simple relationship between the two. To use LST to understand the in-cargo temperatures calls for complex modelling procedures.

4.2.2. Prediction of In-Cargo Relative Humidity (RH)

	Estimate	Standard error	95% confidence interval	
			Lower	Upper
Outside relative humidity	-0.007	0.0013	-0.01	-0.005
Tomato skin temperature	0.019	0.0091	0.001	0.037
Air temperature	-0.02	0.0093	-0.04	-0.002
Constant	5.048	0.104	4.845	5.251
R-Square	0.84			
RMSE	19.59			

Table 4-3 Parameter estimates of in-cargo RH

Table 4-3 above details parameter estimates of the in-cargo RH prediction. The results showed that for every 1% increase in outside RH, there is corresponding 0.007% decrease in the logarithm of the in-cargo RH. Similarly, a 1^0C rise in air temperature led to a decrease of 0.02% in the logarithm of in-cargo RH. A unit rise in the tomato skin temperature is associated with 0.019% increase in the logarithm of the in-cargo RH. At a RMSE of 19.59%, the model explained 84% of the variability in the in-cargo RH. From equation [13], the final predictor equation for the in-cargo RH is given as:

$$\text{Log}\,(RH_{incargo}) = 5.048 - 0.007RH_{out} + 0.019T_{skin} - 0.02T_{air}$$

Equation 29 Final predictor equation for in-cargo relative humidity

The GEE prediction model for the in-cargo RH showed that the determinants of the in-cargo RH are air temperature, outside RH and the tomato skin temperature. All estimated parameters were significant ($P < 0.001$), have low standard errors and the confidence intervals have high coverage rates indicating the robustness of the GEE in fitting the model.

Validation

When the model was validated, a prediction error of 19.59% was found. This relatively high RMSE could be attributed to the intercept term in the model. Though the intercept was found to be significant, a student t-test conducted to test the validity of the model found a systematic error in only the intercept term. However, all the slopes of the predictor variables were found to be significantly different from one implying that the model did not produce bias predictions when the intercept term is dropped (Student T-test, T Slopes = -774.6, -107.8, -109.6. T intercept = 48.5, df = 86, α = 5% t* = 1.66). A zero constant however, could not be assumed for the model because the mechanisms underlying the exchanges of water vapour during the transportation period was beyond the scope of this study and should be discussed elsewhere.

Studies showed that the actual vapour pressure (RH) is temperature dependent (Paull, 1999). This study found this high dependence of RH on temperature as expressed in the air and tomato skin temperatures. The hypothesis test conducted to assess the significance of these associations confirmed that each of the coefficients is significantly different from zero and that a relationship exists between the in-cargo RH and the explanatory variables.

Whereas, both outside RH and air temperatures showed negative association with the in-cargo RH, that of the skin temperature is positive. This is because as the tomato skin temperature increases, there is an increase in the biochemical reactions of the tomato produce and consequently more moisture is released, thereby increasing the in-cargo RH. At the same time, the loss of moisture occasioned by the increased biochemical activity leads to quality deterioration of the produce. From literature, this assertion is supported by Yeshida *et al.* (1984) who observed that high temperatures increase enzymatic catalysis leading to biochemical breakdown of fruits and vegetables and also by Beaudry *et al.* (1992), and Exama *et al.* (1993) who reported that rates of biochemical reactions increases by a factor of 2 or 3 for every 10^0C rise in temperature.

4.2.3. Prediction of in-cargo light intensity

For the in-cargo light intensity, the omission of the intercept term was found to be plausible since light intensity inside the trucks depends sorely on the solar radiation and there was no other source of energy during the transport period. This way, the GEE model did not produce sensible results due to the absence of the intercept. Consequently, simple linear regression model was used and the results are stated in Table 4-4. The equation to predict the in-cargo light intensity formulated in equation [15] is finally given as:

$$LI_{incargo} = 2.29R$$

Equation 30 Final predictor equation for in-cargo light intensity

	Estimate	Standard error	95% confidence interval	
			Lower	Upper
Radiation	2.29	0.092	2.10	2.47
R^2	0.90			
RMSE	137.31			

Table 4-4 Parameter estimates of in-cargo light intensity

Table 4-4 above illustrates the simple linear regression model for the in-cargo light intensity. For every 1Wm^{-2} increase in solar radiation, in-cargo light intensity increases by 2.29Lux. The model showed that the only determinant of the in-cargo light intensity is solar radiation. The variance in in-cargo light intensity explained by the model is 90% at a RMSE of 137.31Lux. The positive association between solar radiation and in-cargo light intensity is expected since there was no other source of energy.

The last three sections have presented the GEE model for the in-cargo temperature and RH and a simple linear regression model for the in-cargo light intensity. The variance explained ranges from 77% for the in-cargo temperature to 90% for the in-cargo light intensity. Plots showing the relationships between the observed and estimated in-cargo micro-climate have been presented in appendix 7.4. These models were developed to predict the in-cargo micro-climate for every 15 minutes interval in a complex dynamic condition for tomatoes in transit based on temporal and spatial predictors.

Based on these results, it can be concluded that the in-cargo micro-climate varies linearly with the outside environmental conditions as stated in the first hypothesis except the LST which exhibited a non-linear relationship. Again, the null hypothesis that the GEE model can be used to predict the in-cargo micro-climate with accurate standard errors and reasonable confidence levels was accepted. However, this can not be said of the in-cargo light intensity where the GEE model failed to yield accurate results. Given different trajectories of outside environmental conditions, the models developed can be used to predict the in-cargo micro-climate under similar situations. The contribution of this study is that it introduces temporal and spatial dimensions to post-harvest quality studies. This kind of study, as far as is known, has never been done.

Although differences in trucks type, colour and dimension can influence in-cargo heat retention, they do not appear to have any significant influence on the in-cargo micro- climate since for a particular truck; these variables don't vary with time. Residual variability in the models can be explained by regular stops of the trucks at security checkpoints and custom controls along the road network. These periodic stops have the potential of altering any dynamic system that might have been established when the truck is in motion. Also differences in the number of tomato crates and the dimensions of the crates in the trucks might also explain part of the residual variability. Ensuring that crates of the same number and dimensions are loaded into the trucks for the different trips could improve the in-cargo micro-climate estimation.

Although the models presented in this study deserves further fine-tuning, the approach presented to predict and map the in-cargo micro-climate experienced by vegetables under various scenarios of outside environmental conditions, appears to be a promising tool in the management of the post-harvest chain and opens new frontiers in the application of Remote sensing and GIS in post-harvest quality studies.

4.3. Quality Evolution model

In section 3.4.5, we proposed a model for the determination of tomato quality evolution during the dynamic transport conditions using analytical equations. Using the solver functionality in excel, optimal solution was found for the model parameters. Table 4-5 below summarizes the results of the parameter optimisation problem:

Parameter	Estimate
aR	0.35361295
bR	0.00226948
aL	4.84776948
bL	0.000015
Kref	0.0075 $hour^{-1}$
Ea	20.411421 $KJmol^{-1}$

Table 4-5 Parameter Estimates of Quality evolution modelling

From equations 23 and 24 above, the analytical equation of firmness loss can then be written as

$$F= 4*\exp(-(0.35361 + 0.002269*RH)*k*(4.847769 + 0.000015*L)*t)$$

Equation 31 Resultant model of the quality model optimization problem

With K according to Arrhenius law as:

$$k= 0.0075*\exp(120.2790474*20.411421*(1 / 293 - 1 / (T + 273)))$$

Equation 32 Arrhenius law with full parameters

The result of the regression analysis with the model output is summarized in Table 4-6 below.

From equation [26] the co-efficient of the vector of the explanatory variables was found to be 0.655 with a standard error of 0.057. Equation 26 is then reported as

$$y = 0.655(X, P)$$

Equation 33 Final equation of the quality evolution modelling

X and P can now be represented by, equations [31] and [32].

Table 4-6 Summary Statistics of Quality Evolution Model

Regression Statistics	
Multiple R	0.878
R square	0.771
Adjusted R square	0.745
Estimate	0.655
Standard error	0.057
Observations	40
N for Validation	25

From Table 4-6 above, the developed quality evolution model explained 77% of the variability in the observed firmness. Also from Table 4-5, under the combined effect of all the explanatory variables, the firmness of tomatoes decreased exponentially during the course of transportation with a reference rate constant of 0.0075hour^{-1} (1.25 X 10^{-4}min^{-1}) and activation energy of 20.411KJmol^{-1}. This result, though consistent with the results found by Lana *et al.* (2005) - who explained that tomato slice firmness decreased exponentially during storage with a reference rate constant of 0.0975 ± 0.0183 day^{-1} - is still significantly higher than the firmness decay reported by Lana *et al.* (2005)

Validation

The validation process was performed by comparing the estimated and observed firmness along the transportation route. For this, the standard deviation and the student t –test were used to assess how well the estimated firmness approaches the observed firmness. The mean observed firmness for the validation data was found to be 1.44Kg whilst the average estimated firmness of the simulations at any trajectory of the predictors was found to be 0.96Kg with a standard deviation of 0.53Kg. A cursory look at the results also indicates that the firmness decay during the entire transportation period is approximately 30% of the firmness levels at the start of the transportation. This result obtained from the quality evolution modelling is consistent with visual observation at destination points which revealed that between 30-40% of the tomatoes were not acceptable for consumers either as a result of being too soft or lacking some other important quality attribute. Moreover, Auerswald *et al.* (1999) also found that the finger touch firmness of tomatoes decayed from 67.8 to 40.9 (40%) at the end of 7 days.

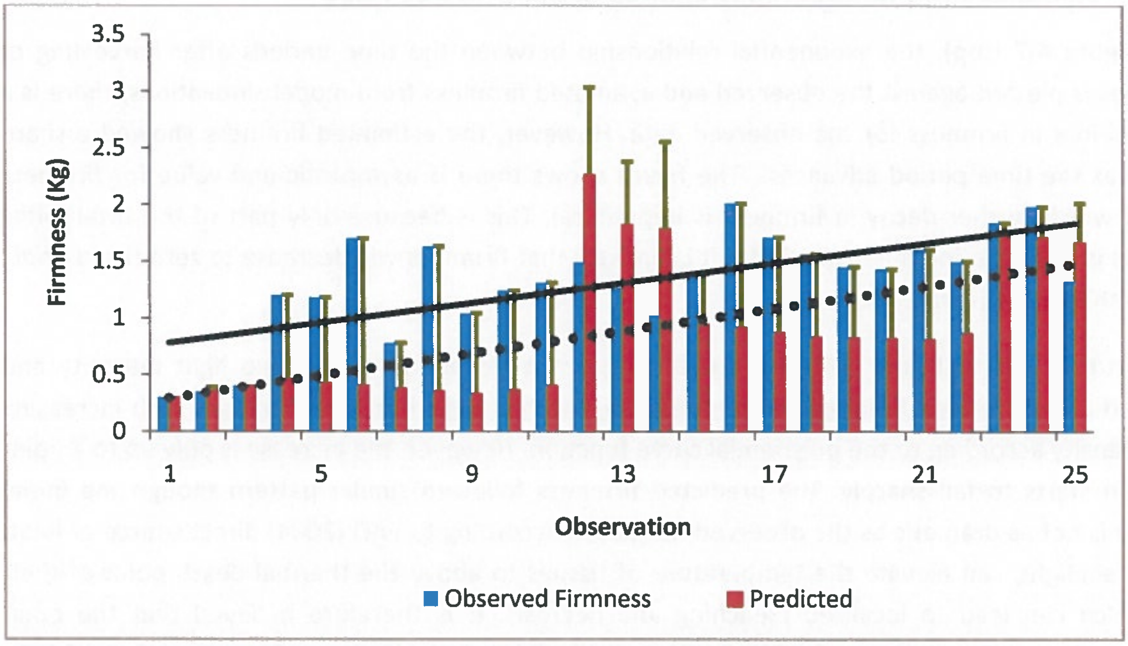

Figure 4-6 Error bars of estimated firmness from the optimised estimates in equations [32] and [33].
Solid line = observed firmness trend line; Dotted line = estimated firmness

In Figure 4-6, the observed and estimated firmness for all validation are shown. The plot shows a linear association between the observed firmness and the model outputs as indicated by the two linear trend lines. The error bars indicate the deviation of the estimated firmness from the observed firmness. Though some of the error amounts are quite acceptable, some seem large. This is due to the scattering of the validation data itself. Because of the destructive nature of the penetrometer used to measure the firmness, evaluated tomatoes were immediately discarded. The use of new tomato for each evaluation was necessary to exclude the negative effect of manual contact and also the destruction caused by the penetrometer. This method will no doubt account for some variability in the firmness values. Appendix 7.2 shows the normal probability plot of the regression analysis.

To further test the validity of the firmness decay model, use was made of the student t-test. For a perfect predictor, the diagonal in a regression line should have equation of the form Y = 0 + 1.X. Since the intercept term has already been dropped, here, the only assessment is whether the slope is indeed equal to one for the model to be considered a perfect predictor. The hypothesis is thus formulated as follows:

Ho: $\beta = 1$ and Ha: $\beta \neq 1$

Where β is the slope of the vector of the model parameters stated in Equation (33). Applying the formula in equation [28] and using a standard error of 0.057 yielded a calculated t-value of -6.05. The critical t value at $\alpha = 0.05$ and at 22 degrees of freedom was obtained as 1.725 from the t distribution critical values table. Since the observed t value is less than the expected t value, we fail to reject the null hypothesis that states the slope is equal to one and conclude that the firmness decay model did not produce bias predictions and that it is free from systematic error or bias (Student T-test, T Slopes -6.05, df = 24, α = 5%, t^* = 1.73)

4.3.1. Dynamics of In-cargo micro-climate and Firmness Loss

From Figure 4-7 (top), the exponential relationship between the time periods after harvesting of tomatoes is plotted against the observed and estimated firmness from model simulations, there is a marginal loss in firmness for the observed data. However, the estimated firmness showed a sharp decline as the time period advances. The figure shows there is asymptotic end value for firmness beyond which further decay in firmness is impractical. This is because only part of the total initial firmness is available for change and that it is unlikely that firmness will decrease to zero (Lana *et al.*, 2005; Van Dijk & Tijskens, 2000).

The bottom chart in Figure 4-7 shows the relationship between the in-cargo light intensity and observed and estimated firmness. As can be seen, the observed firmness increases with increasing light intensity according to the polynomial curve function. However, the increase is only up to a point and then starts to fall sharply. The predicted firmness followed similar pattern though the initial increase is not as dramatic as the observed firmness. According to FAO (2004) direct source of heat, such as sunlight, can elevate the temperature of tissues to above the thermal death point of their cells which can lead to localized bleaching and necrosis. It is therefore believed that the open transportation system used in the study area could affect the tomato quality. The effect of light intensity on tomato firmness is not well understood but according to Paull (1999) warm fruits are generally more plastic and better able to withstand impact injury. This explains why the both the observed and estimated firmness increases with increasing light intensity because the fruits gets warmer. However, as the light intensity increases above 5000 Lux, the fruits are no longer able to withstand the intense heat probably due to attainment of their thermal death points and consequently there is accelerated firmness decay.

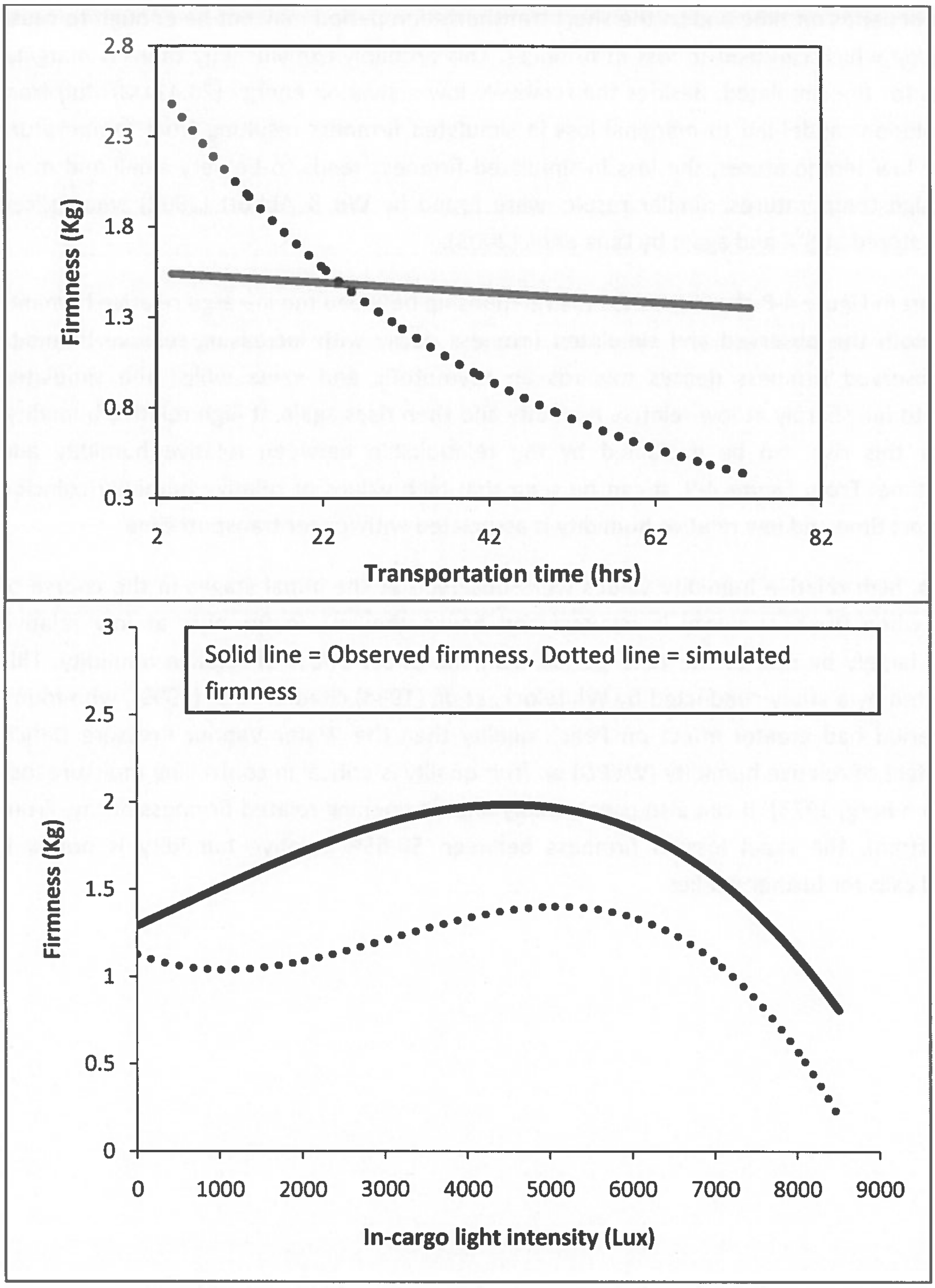

Figure 4-7 Relationship between firmness and the predictor variables

- *Top: Relation between transport time, observed firmness and simulated firmness derived from the quality evolution models.*

  Bottom: In-cargo light intensity versus observed and estimated firmness of tomatoes.

For the in-cargo temperature, (Figure 4-8, top) the observed firmness rises slightly as the temperature moves from 22^{0}C to 42^{0}C. However, the exponential function showed a rather opposite result for the simulated firmness, though the change is only marginal. Paull (1999) found out that storage temperature can significantly affect fruit firmness and the loss increases with storage time. This loss, nevertheless, is related more to ripening than the direct effect of temperature on firmness (Miccolis & Saltveit, 1995). For a climacteric fruit like tomatoes, the rate of ripening during post-harvest largely depends on time and so the short transportation period may not be enough to cause excessive ripening which can lead to loss in firmness. This probably explains why there is marginal loss in firmness for the simulated. Besides the relatively low activation energy (20.411KJ/Mol) from the quality evolution model led to marginal loss in simulated firmness resulting from temperature fluctuations. At low temperatures, the loss in simulated firmness tends to be very small and more noticeable at high temperatures. Similar results were found by Wu & Abbott (2002) when sliced tomatoes were stored at 5^0C and again by Lana *et al.* (2005).

The bottom chart in Figure 4-8 also illustrates the relationship between the in-cargo relative humidity and firmness. Both the observed and simulated firmness decay with increasing relative humidity though, the observed firmness decays towards an asymptotic end value whilst the simulated firmness tends to fall sharply at low relative humidity and then rises again at high relative humidity. The reason for this rise can be explained by the relationship between relative humidity and transportation time. From Figure 4-9, it can be seen that high values of relative humidity coincide with low transport time and low relative humidity is associated with longer transport time.

In simple terms, high relative humidity values were observed at the initial stages in the course of transportation when firmness decay is minimal and hence the loss in firmness at low relative humidity could largely be due to the time period than the direct effect of relative humidity. This result is supported by a study conducted by Whitelock, *et al.* (1994) cited in Paull (1999), who found that storage period had greater effect on Peach quality than the Water Vapour Pressure Deficit (WVPD). The effect of relative humidity (WVPD) on fruit quality is critical in controlling moisture loss (Lentz & Van Den Berg, 1973). It can also considerably impact ripening related firmness decay. From Figure 4-8 (bottom), the rapid loss in firmness between 50-65% relative humidity is not well understood and calls for further studies.

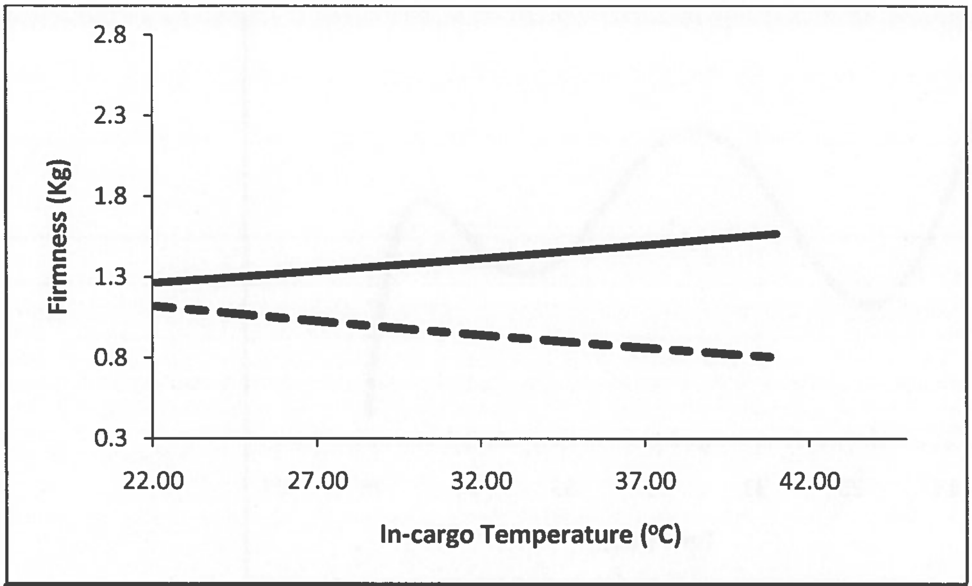

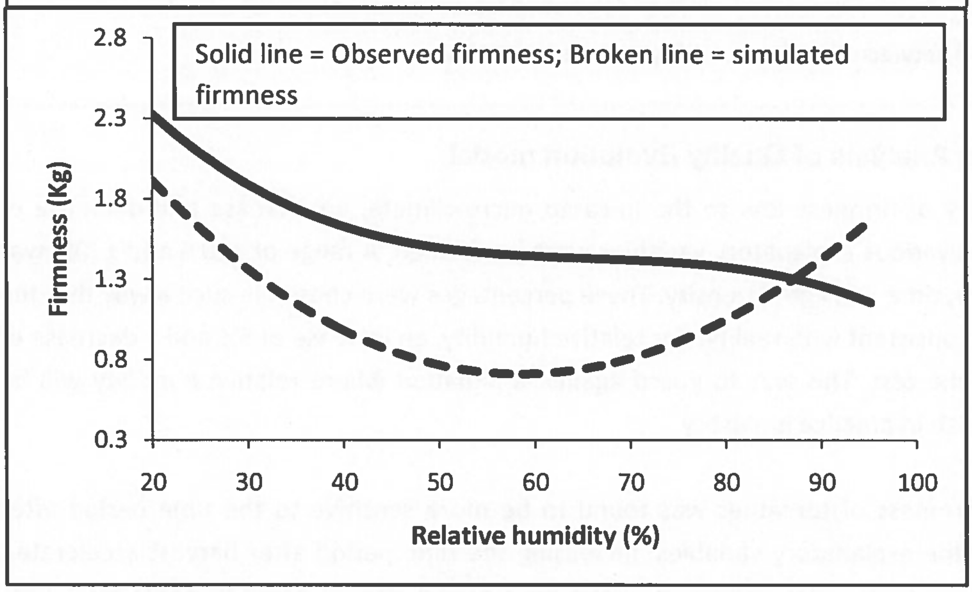

Figure 4-8 Relationship between firmness and two explanatory variables
Top: In-cargo temperature versus observed and estimated firmness of tomatoes

Bottom: In-cargo relative humidity versus observed and estimated firmness.

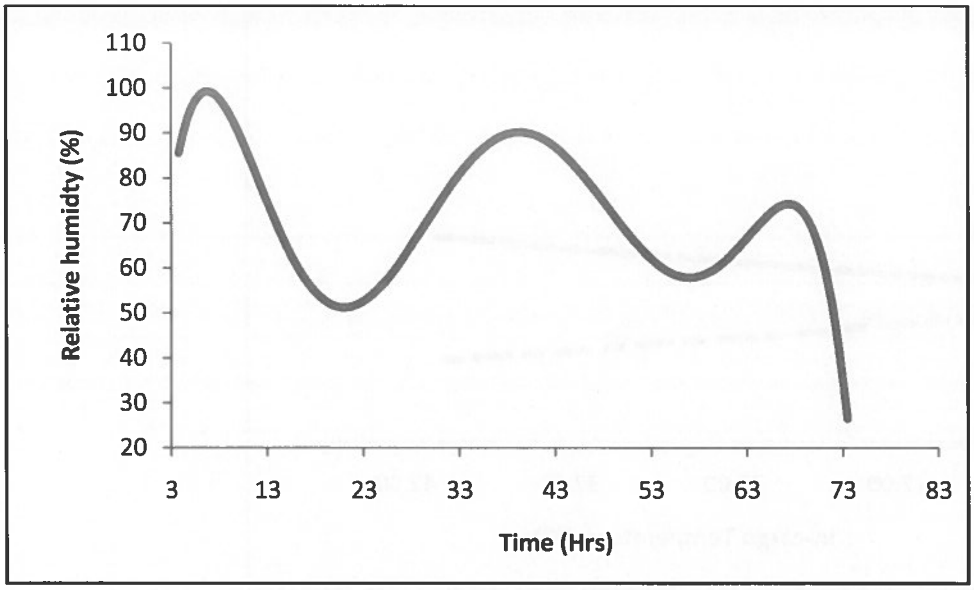

Figure 4-9 Relationship between Relative humidity and transport time

4.3.2. Sensitivity Analysis of Quality Evolution model

To test the sensitivity of firmness loss to the in-cargo micro-climate, an increase and decrease of varying ranges of the various explanatory variables were performed. A range of ±10% and ±30% was used for temperature, time and light intensity. These percentages were chosen in such a way that the values obtained are consistent with reality. For relative humidity, an increase of 5% and a decrease of 30% were used for the test. This was to guard against a situation where relative humidity will be more than 100%, which in practice is illusory.

From Figure 4-10, firmness of tomatoes was found to be more sensitive to the time period after harvest than any of the explanatory variables. Increasing the time period after harvest accelerated firmness loss by 2.2% whilst a 10% reduction in the time period slowed down firmness by 2.23%. Similarly, a 30% delay in transportation time increased firmness loss by 6.5% whilst a corresponding 30% improvement in transport time slowed firmness decay by 7.03%. The next sensitive parameter to firmness decay is temperature. An increase of 10% in the in-cargo temperature reduces firmness loss rate by 1.76% whilst a 30% increase led to 5.46% decreases in firmness loss.

The next most important determinant of tomato quality is relative humidity. Interestingly, decreasing relative humidity by 30% rather improved firmness by 2.35%. This trend can be understood by referring to a study conducted by Paull (1999) who observed that high RH will not prevent moisture loss which could lead to a loss in firmness if the product temperature (skin temperature) is not near the air temperature.

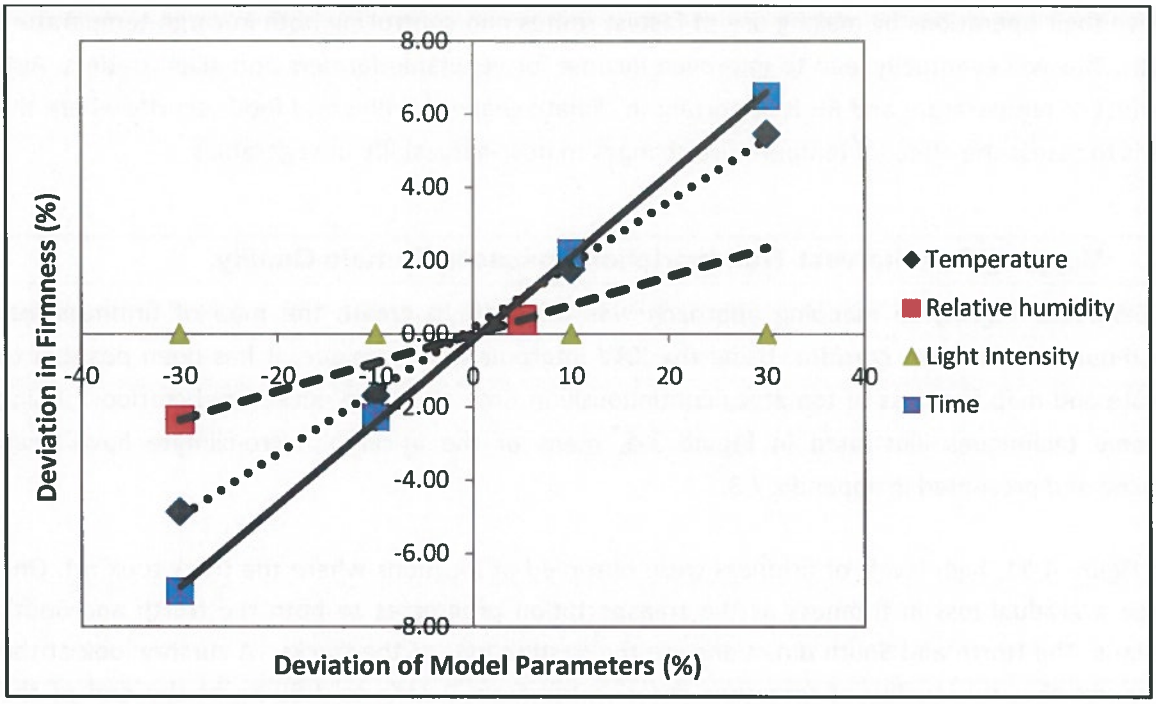

Figure 4-10 Sensitivity analysis of model variables on Tomato firmness loss

A look at the relationship between the tomato skin temperature and ambient temperature (appendix 7.2 (right) showed that the tomato skin temperature is well below the air temperature. It is thus true that though RH can increase, even up to 95%, firmness loss will continue unabated because of the difference between the tomato skin temperature and air temperature. It is however not well understood why firmness loss is reduced as RH falls. Firmness of tomatoes virtually seems to be insensitive to fluctuation in light intensity though Figure 4-7 (bottom) showed a relationship between the two. This could well be due to the fact that the tomato trucks travelled mostly at night and so the stream of light intensity values to which the tomatoes were subjected to was limited. It is thus probable that this effect of light intensity on tomato quality can change under full stream of light intensity values, thus when the trucks travel during the day rather than night.

From the discussions above, it was established that the firmness of tomatoes decreases exponentially during the transportation period. The relationships between firmness and the predictor variables have been succinctly outlined. The null hypothesis that the open transportation system used in the study area has significant detrimental effects on the quality of tomatoes is thus accepted. Also the quality evolution model developed to predict the firmness decay during the dynamic condition in transport explained 77% of the variability in the firmness. It therefore follows that the quality of tomatoes under such a transportation system depends largely on the in-cargo micro-climate proposed in this study and that only 23% could be due to other external factors which were not considered. It is however, believed that this residual variability primarily resulted from the method and instrument used to evaluate the tomato quality rather than the presence of any lurking variable.

These results are important for the development of efficient post-harvest management in the horticultural industry in West Africa. Reducing transport time and temperature have been found to result in quality optimization. The horticultural chain industry can take advantage of these findings to improve their operations by making use of fastest routes and controlling both in-cargo temperature and RH. This will eventually lead to improved income for vegetable farmers and allied traders. Also the effect of temperature and RH is important in climate change studies and food security where the focus is to assess the effect of temperature changes to post-harvest life of vegetables.

4.3.3. Mapping Post-harvest Transportation Losses in Tomato Quality.

The GIS-based regression mapping approach was followed to create the map of firmness loss throughout the transport corridor. Using the IDW interpolation technique, it has been possible to estimate and map firmness of tomatoes continuously in time along the entire road corridor. Using the same techniques illustrated in Figure 3-5, maps of the in-cargo micro-climate have been produced and presented in appendix 7.3.

From Figure 4-11, high levels of firmness were observed at locations where the truck took off. One can see a gradual loss in firmness as the transportation progresses to both the North and South directions. The North and South directions are the destinations of the trucks. A cursory look at the map shows that the quality of tomatoes deteriorated from 2.34Kg to 1.65 Kg at the end of the transportation representing 30% lost in quality.

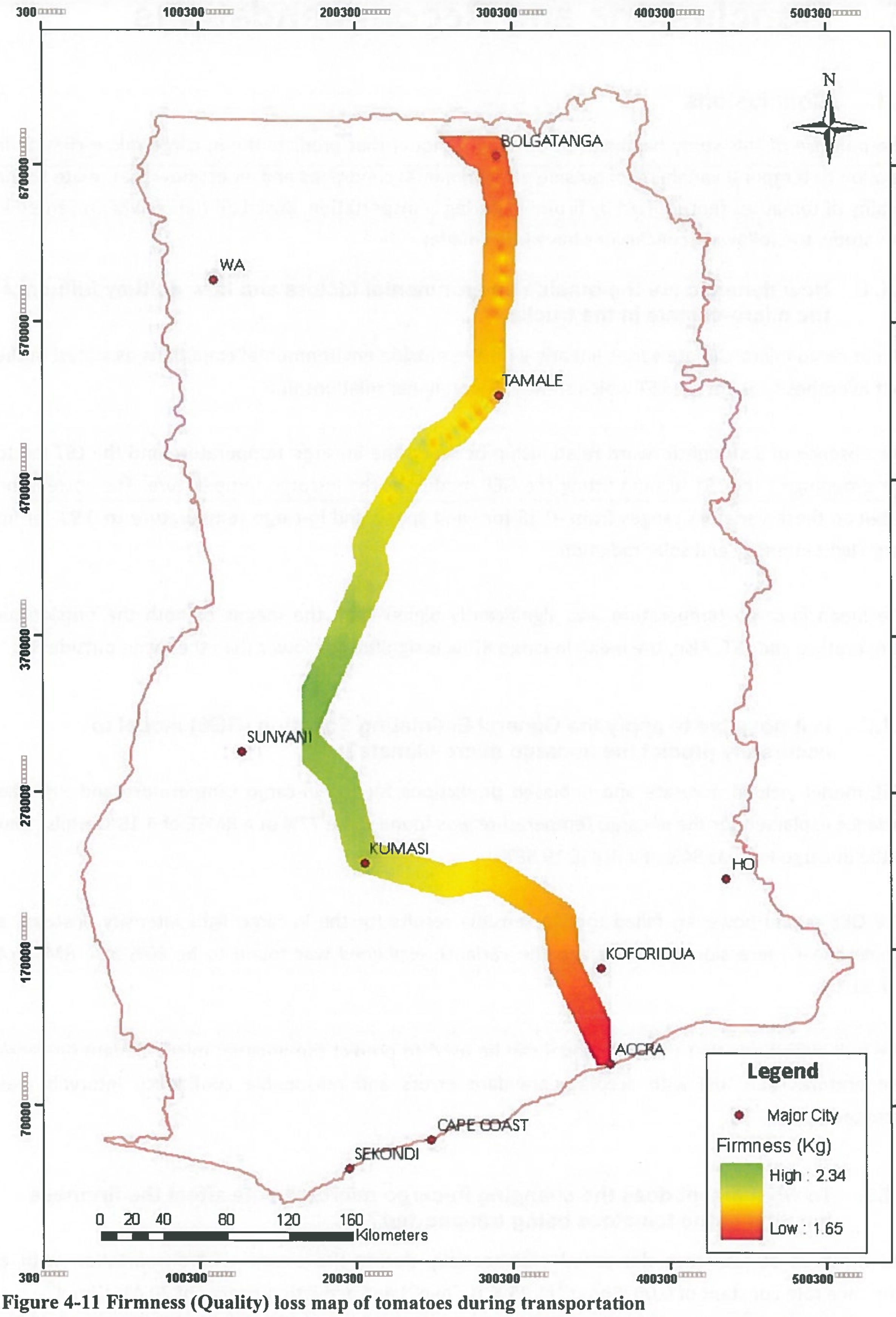

Figure 4-11 Firmness (Quality) loss map of tomatoes during transportation

Note that the truck took off in the middle of the road close to the city, Sunyani. Truck 1 and 3 moved in the North direction whilst truck 1 moved towards the South, i.e. to the coastal city of Accra. In both directions, there was gradual loss in firmness.

5. Conclusions and Recommendations

5.1. Conclusions

The purpose of this study has been to develop a model that predicts the in-cargo micro-climate in relation to temporal variability of outside environmental conditions and assess how that relate to the quality of tomatoes represented by firmness during transportation. Based on the results presented in this study, the following conclusions have been made:

5.1.1. How dynamic are the outside environmental factors and how do they influence the micro-climate in the trucks?

The in-cargo micro-climate varies linearly with the outside environmental conditions as stated in the first hypothesis except the LST which showed a non-linear relationship.

The absence of a straightforward relationship between the in-cargo temperature and the LST led to the dropping of the LST term in fitting the GEE model for the in-cargo temperature. The correlation between these variables ranges from -0.36 for wind speed and in-cargo temperature to 0.91 for in-cargo light intensity and solar radiation.

The mean in-cargo temperature was significantly higher than the means of both the outside air temperature and LST. Also, the mean in-cargo RH was significantly lower than the mean outside RH.

5.1.2. Is it possible to apply the General Estimating Equation (GEE) model to accurately predict the in-cargo micro-climate?

GEE model yielded accurate and unbiased predictions for the in-cargo temperature and RH. The variance explained for the in-cargo temperature was found to be 77% at a RMSE of 4.18^{0}C whilst that of the in-cargo RH was 84% at a RMSE 19.59%.

The GEE model however, failed to give sensible results for the in-cargo light intensity. Instead, a simple linear regression was used and the variance explained was found to be 90% at a RMSE of 137.31Lux.

The null hypothesis that the GEE model can be used to predict the in-cargo micro-climate (in-cargo temperatures and RH) with accurate standard errors and reasonable confidence intervals was accepted.

5.1.3. To what extent does the changing in-cargo micro-climate affect the firmness (quality) of the tomatoes being transported?

The firmness of tomatoes decreased exponentially during the course of transportation with a reference rate constant of 0.0075hour^{-1} (1.25 X 10^{-4}min^{-1}) and activation energy of 20.411KJmol^{-1}.

The average estimated firmness of the simulations at any trajectory of the explanatory variables was found to be 0.96 ±0.53Kg.

The quality evolution model using analytical equations for constant conditions developed to predict the firmness decay during the dynamic condition in transport explained 77% of the variability in the tomato firmness.

The 23% residual variability in observed firmness could be due to other external factors which were not considered. It is however, believed that this residual variability primarily resulted from the method and instrument used to evaluate the tomato quality rather than the presence of any lurking variable.

The quality of tomatoes under such a transportation system depends largely on the in-cargo micro-climate of temperature, RH, light intensity and the time period after harvest.

5.1.4. How sensitive is the tomato quality to fluctuations in the in-cargo- micro climate?

The quality of tomato fruits was found to be more sensitive to the time period after harvest than any of the explanatory variables. Delaying the time period after harvest by 10% and 30% led to firmness losses of respectively 2.2% and 6.5%. The next most important sensitive parameter to firmness loss was temperature.

Tomato firmness was insensitive to the in-cargo light intensity. This could be due the low stream of values of light intensity to which the tomatoes were subjected because the trucks travelled mostly at night.

Reducing transport time, controlling temperature and RH have been found to result in quality optimization and a reduction in the firmness loss.

It was possible to use the GIS-based regression mapping approach to map the quality of tomatoes continuously in time throughout the transportation.

5.2. Recommendations

The number of sensors used to sample the in-cargo micro-climate was few compelling data collection at limited layers within the truck based on the assumption made on the system boundary. It would be appropriate to further test this assumption and should the need be, use more sensors so that the various compartments within the truck could be sampled.

For lack of time, tomato trucks that travelled mostly at night were sampled. It would be useful to use trucks that travel both day and night. For instance the use of night trucks means that, only limited data points for the light intensity simulations could be used.

More importantly, the inability to sample more quality evaluations on the actual truck necessitated the need to use tomato quality data from simulated truck conditions in pick-up vehicles and climate chamber. Avenues to ensure that quality data are obtained on the trucks themselves should be explored.

The destructive nature of the penetrometer used to measure the firmness meant that evaluated tomatoes had to be immediately discarded. The use of new tomato for each evaluation accounted for some variability in the observed firmness. We recommend that non-destructive methods of evaluating the quality of the tomato should be used in subsequent studies.

Since this study appears to be the first of its kind in this field, further studies are also recommended on especially the fitted GEE models and the quality evolution model in order to gain further understanding of this complex system. The study should also explore ways of translating the quality losses into economic losses to actors along the post-harvest chain.

Although the models presented in this study deserve further fine-tuning, the approach presented to predict and map the in-cargo micro-climate experienced by vegetables under various scenarios of outside environmental conditions, appear to be promising tools in the management of the post-harvest chain and opens new frontiers in the application of Remote sensing and GIS in post-harvest quality studies. It is also especially, applicable to climate change studies where the focus will be to study the effects of temperature, RH and solar radiation variability to regional or global food security issues resulting from post-harvest management of fruits and vegetables.

Total 62 References → means nearly Av $\frac{62}{8} \approx 8$ literature / month
means should be nearly min 20 ~~literature~~ Reference at proposal

References

Abbott, J. A. (1999). Quality measurement of fruits and vegetables. *Postharvest Biology and Technology*, 15(3), 207-225.

Ali, B. (1998). Some Factors Affecting on Determination and Measurement of Tomato Firmness. *Turkish journal of Agriculture and Forestry*(22), 411-418.

Auerswald, H., Peters, P., Brückner, B., Krumbein, A.& Kuchenbuch, R. (1999). Sensory analysis and instrumental measurements of short-term stored tomatoes (Lycopersicon esculentum Mill.). *Postharvest Biology and Technology*, 15(3), 323-334.

AVRDC. (2006). Training Manual on Postharvest Research and Technology Development for Tomato and Chilli in RETA 6208 Countries. Paper presented at the RETA 6208 Training-Workshop on Postharvest Research and Technology Development, Lao PDR.

Bastin, G.& Dochain, D. (1990). On-line estimation and adaptive control of bioreactors. Amsterdam, The Netherlands: Elsevier Science Publisher.

Beaudry, R. M., Cameron, A. C., Shirazi, A.& Lange, D. D. (1992). Modified atmosphere packaging of blueberry fruit: effect of temperature on package oxygen and carbon dioxide. *J. Am. Soc. Horticulture*, 117, 431-436.

Becker, F.& Li, Z. L. (1990). Toward a local split window method over land surface. International *Journal of Remote Sensing*, 11, 369-393.

Carl, G.& Kühn, I. (2007). Analyzing spatial autocorrelation in species distributions using Gaussian and logit models. *Ecological Modelling*, 207(2-4), 159-170.

Castro, L. R., Vigneault, C., Charles, M. T.& Cortez, L. A. (2005). Effect of cooling delay and cold-chain breakage on 'Santa Clara' tomato. *Journal of Food Agriculture and Environment*, 3, 49-54.

Chang, K. (2004). Introduction to geographic information systems (2nd edition). New York, NY 10020: McGraw Hill companies.

Cumba, R. D. (2006). Temporal dynamics in radiation and temperature and its influence on CO2 crops assimilation. ITC, Enschede.

De Lucia, M.& Assennato, D. (1994). Agricultural engineering in development: post-harvest operations and management of food grains (Publication. Retrieved August 10, 2008, from FAO: http://www.fao.org/inpho/pp-dr/pp-arch/full-doc/frame-e.htm

Doraiswamy, P. C., Hatfield, J. L., Jackson, T. J., Akhmedov, B., Prueger, J.& Stern, A. (2004). Crop condition and yield simulations using Landsat and MODIS. Remote Sensing of Environment, 92(4), 548-559.

EUMETSAT. (2006). A short introduction to Meteosat Second Generation (MSG). MSG CHANNELS Interpretation Guide Weather, surface conditions and atmospheric constituents Retrieved August 7, 2008, from http://oiswww.eumetsat.org/WEBOPS/msg_interpretation/index.html

Exama, A., Arul, J., Lencki, R. W., Lee, L. Z.& Toupin, C. (1993). Suitability of plastic films for modified atmosphere packaging of fruits and vegetables. *Journal of food Science*, 58, 1365-1370.

FAO. (1989). Prevention of post-harvest food losses fruits, vegetables and root crops, a training manual (Vol. II). Rome: Food and Agriculture Organization of the United Nations.

FAO. (2004). The role of post-harvest management in assuring the quality and safety of horticultural produce FAO Agricultural Services Bulletins - 152 Retrieved 20th May, 2008, from http://www.fao.org/docrep/007/y5431e/y5431e06.htm

FAO. (2006, 30 January – 3 February). Enhancing the Competitiveness of Agriculture and Natural Resource Management under Globalization and Liberalization to Promote Economic Growth. Paper presented at the Twenty-Fourth Regional Conference for Africa, Bamako, Mali.

Fonseca, S. C., Oliveira, F. A. R.& Brecht, J. K. (2002). Modelling respiration rate of fresh fruits and vegetables for modified atmosphere packages: a review. *Journal of Food Engineering*, 52(2), 99-119.

Getinet, H., Seyoum, T.& Woldetsadik, K. (2008). The effect of cultivar, maturity stage and storage environment on quality of tomatoes. *Journal of Food Engineering*, 87(4), 467-478.

Halekoh, U., Hojsgaard, S.& Yan, J. (2006). The R Package geepack for Generalized Estimating Equations. *Journal of Statistical Software*, 15(2), 11.

Hammer, A., Heinemann, D., Hoyer, C., Kuhlemann, R., Lorenz, E., Müller, R.& Beyer, H. G. (2003). Solar energy assessment using remote sensing technologies. *Remote Sensing of Environment*, 86(3), 423-432.

Hanley, J. A., Negassa, A., Edwardes, M. D. d.& Forrester, J. E. (2003). Statistical Analysis of Correlated Data Using Generalized Estimating Equations: An Orientation. *Am. J. Epidemiol.*, 157(4), 364-375.

Lana, M. M., Tijskens, L. M. M.& Kooten, O. v. (2005). Effects of storage temperature and fruit ripening on firmness of fresh cut tomatoes. *Postharvest Biology and Technology*, 35(1), 87-95.

Lana, M. M., Tijskens, L. M. M.& van Kooten, O. (2006). Effects of storage temperature and stage of ripening on RGB colour aspects of fresh-cut tomato pericarp using video image analysis. *Journal of Food Engineering*, 77(4), 871-879.

Lefe`vre, M., Albuisson, M.& Wald, L. (2002). Joint report on interpolation scheme 'meteosat' and database 'climatology' i (meteosat). Technical report: Report for the European Commission.

Lentz, C. P.& Van Den Berg, L. (1973). Factors affecting temperature, relative humidity and moisture loss in fresh fruit and vegetable storage. *American Soc. Heating Refrigeration and Air Conditioning* 15, 55-60.

Liang, K.-Y.& Zeger, S. L. (1986). Longitudinal Data Analysis Using Generalized Linear Models. *Biometrika*, 73(1), 13-22.

Lukasse, L. J. S.& Polderdijk, J. J. (2003). Predictive modelling of post-harvest quality evolution in perishables, applied to mushrooms. *Journal of Food Engineering*, 59(2-3), 191-198.

McCullagh, P.& Nelder, J. A. (1983). Generalized Linear Models. London: Chapman and Hall.

Miccolis, V.& Saltveit, M. E. (1995). Influence of storage temperature on postharvest characteristics of six melons (Cucumis melo L., Inodorus Group) cultivars. *Postharvest Biology and Technology*, 5, 211-219.

Mizrach, A. (2008). Ultrasonic technology for quality evaluation of fresh fruit and vegetables in pre- and postharvest processes. *Postharvest Biology and Technology*, 48(3), 315-330.

Moore, D. S., McCabe, G. P.& Craig, B. A. (2009). Introduction to the practice of statistics (Sixth ed.). New York: W. H. Freeman and Company.

Mostovoy, G., King, R., Reddy, K., Kakani, V.& Filippova, M. (2006). Statistical Estimation of Daily Maximum and Minimum Air Temperatures from MODIS LST Data over the State of Mississippi. *GIScience & Remote Sensing*, 43(1), 78-110.

Mueller, R. W., Dagestad, K. F., Ineichen, P., Schroedter-Homscheidt, M., Cros, S., Dumortier, D., Kuhlemann, R.et al. (2004). Rethinking satellite-based solar irradiance modelling: The SOLIS clear-sky module. *Remote Sensing of Environment*, 91(2), 160-174.

Murray, D., McWhirter, J., Wier, S.& Emmerson, S. (2003). The Integrated Data Viewer: a Web-enabled application for scientific analysis and visualization. Paper presented at the 19th Intl Conf. on IIPS for Meteorology, Oceanography and Hydrology.

New Agriculturist. (2005). From crops to shops: improving the post-harvest sector. Retrieved August, 4, 2008, from http://www.new-agri.co.uk/99-5/develop/dev04.html

Paull, R. E. (1999). Effect of temperature and relative humidity on fresh commodity quality. *Postharvest Biology and Technology*, 15(3), 263-277.

Peres, L. F.& DaCamara, C. C. (2004). Land surface temperature and emissivity estimation based on the two-temperature method: sensitivity analysis using simulated MSG/SEVIRI data. *Remote Sensing of Environment*, 91(3-4), 377-389.

Perez, R., Renne, D., Seals, R.& Zelenka, A. (1998). The strength of satellite-based solar resource assessment. Production of site/time specific irradiances from satellite and ground data. New York: New York State Energy Research and Development Authority, Corporate. (W. E. E. Plaza West, Albany, NY,12203-6399.

Porter, W. P., Mitchel, J. W., Beckman, W. A.& DeWitt, C. B. (1973). Behavioral Implications of Mechanistic Ecology. Thermal and Behavioral of Desert Ectotherms and their Microenvironment. *Oecologia*, 13, 1-54.

Qiao, J., Sasao, A., Shibusawa, S., Kondo, N.& Morimoto, E. (2005). Mapping Yield and Quality using the Mobile Fruit Grading Robot. *Biosystems Engineering*, 90(2), 135-142.

Schouten, R. E., Huijben, T. P. M., Tijskens, L. M. M.& van Kooten, O. (2007). Modelling quality attributes of truss tomatoes: Linking colour and firmness maturity. *Postharvest Biology and Technology*, 45(3), 298-306.

Schroedter-Homscheidt, M., Drews, A.& Heise, S. (2008). Total water vapor column retrieval from MSG-SEVIRI split window measurements exploiting the daily cycle of land surface temperatures. *Remote Sensing of Environment*, 112(1), 249-258.

Smargiassi, A., Fournier, M., Griot, C., Baudouin, Y.& Kosatsky, T. (2008). Prediction of the indoor temperatures of an urban area with an in-time regression mapping approach. *Journal of Exposure Science and Environmental Epidemiology*, 18(3), 282-288.

Stisen, S., Sandholt, I., Nørgaard, A., Fensholt, R.& Eklundh, L. (2007). Estimation of diurnal air temperature using MSG SEVIRI data in West Africa. *Remote Sensing of Environment*, 110(2), 262-274.

Sun, D.& Pinker, R. T. (2007). Retrieval of surface temperature from the MSG-SEVIRI observations: Part I. Methodology. *International Journal of Remote Sensing*, 28(23), 5255-5272.

Sun, D. L.& Pinker, R. T. (2003). Estimation of land surface temperature from a Geostationary Operational Environmental Satellite (GOES-8). *Journal of Geophysical Research-Atmospheres*, 108(D11).

Tano, K., Oulé, M. K., Doyon, G., Lencki, R. W.& Arul, J. (2007). Comparative evaluation of the effect of storage temperature fluctuation on modified atmosphere packages of selected fruit and vegetables. *Postharvest Biology and Technology*, 46(3), 212-221.

Tijskens, L. M. M., Veltman, R. H., Heuvelink, E.& Simˇciˇc, M. (2002). Modelling postharvest quality behaviour as affected by pre-harvest conditions. *Acta Horticulture*, 599(469-477).

USAID. (2008). Improved Road Transport Governance Project, IRTG. Report of January 1 – June 15, 2008. Retrieved from: www.irtg.watradehub.com.

Van Dijk, C., Boeriu, C., Peter, F., Stolle-Smits, T.& Tijskens, L. M. M. (2006). The firmness of stored tomatoes (cv. Tradiro). 1. Kinetic and near infrared models to describe firmness and moisture loss. *Journal of Food Engineering*, 77(3), 575-584.

Van Dijk, C.& Tijskens, L. M. M. (2000). Mathematical modelling of enzymatic reactions as related to texture after storage and mild preheat treatment: In S. M. Alzamora, M. S. Tapia, & A. Lopez-Malo (Eds.), Minimally processed fruits and vegetables. Maryland, USA: Aspen Publishers.

Verbyla, D. L.& Litvaitis, J. A. (1989). Resampling methods for evaluating classification accuracy of wildlife habitat models. *Environmental Management*, 13, 783-787.

Whitelock, D. P., Brusewitz, G. H., Smith, M. W.& Zhang, X. H. (1994). Humidity and air flow during storage affect peach quality In:Effect of temperature and relative humidity on fresh commodity quality. *Postharvest Biology and Technology*, 15, 263-277.

Wu, T.& Abbott, J. A. (2002). Firmness and force relaxation characteristics of tomatoes stored intact or as slices. *Postharvest Biology and Technology*, 24, 59-68.

Yáñez, F. F. (2007). Thermoregulation and use of Microhabitat by Timon lepidus (Daudin, 1802). ITC, Enschede.

Yang, K., Koike, T.& Ye, B. (2006). Improving estimation of hourly, daily, and monthly solar radiation by importing global data sets. *Agricultural and Forest Meteorology*, 137(1-2), 43-55.

Yeshida, O., Nakagaua, H., Ogura, N.& Sato. (1984). Effect of heat treatment on the development of polygalacturonase activity in tomato fruit during ripening. *Plant Cell Physiology*, 25(3), 500-509.

Zeger, S. L.& Liang, K.-Y. (1986). Longitudinal Data Analysis for Discrete and Continuous Outcomes. *Biometrics*, 42(1), 121-130.

Zeger, S. L., Liang, K.-Y.& Albert, P. S. (1988). Models for Longitudinal Data: A Generalized Estimating Equation Approach. *Biometrics*, 44(4), 1049-1060.

Zelenka, A., Perez, R., Seals, R.& Renne, D. (1999). Effective accuracy of satellite derived hourly irradiances. *Theoretical and Applied Climatology*, 62, 199– 207.

Appendices

Appendix 7.1 System Boundary

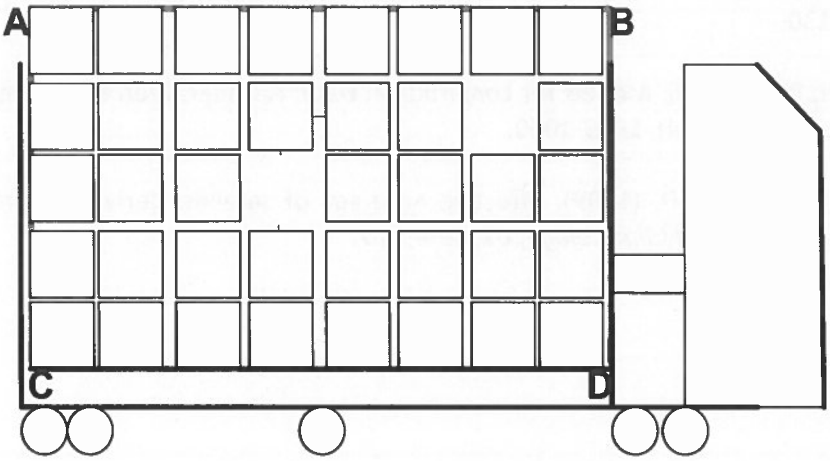

The rectangle ABCD is the system boundary and any phenomenon outside this rectangle is beyond the boundary of the in-cargo micro-climate. The two measurements were found to be more or less match each other indicating that in-cargo micro-climate fall just on top of the crates beyond which is the domain of outside environmental conditions. The dimensions of the crates were 6ocm x 60cm. The net crate dimension, i.e. excluding the thickness of the wood that was used to construct the crate was also 58cm x 58cm. The implication is that the wooden material is only 2cm thick and thus can be considered to have little effect on the in-cargo microclimate.

Appendix 7.2: Normal probability plot and relationship between air and Tomato skin temperatures

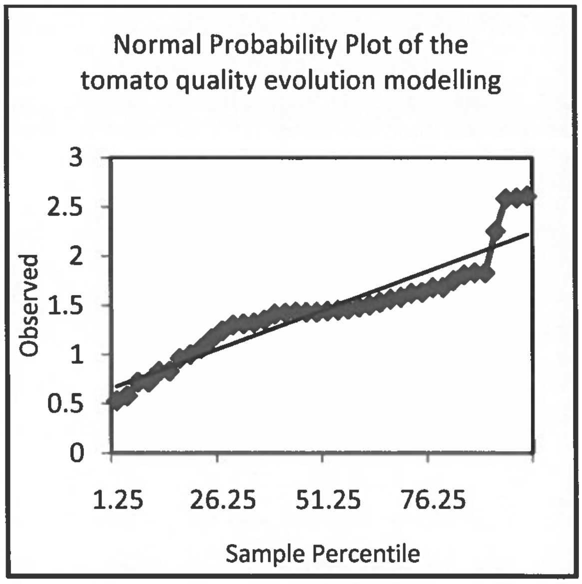

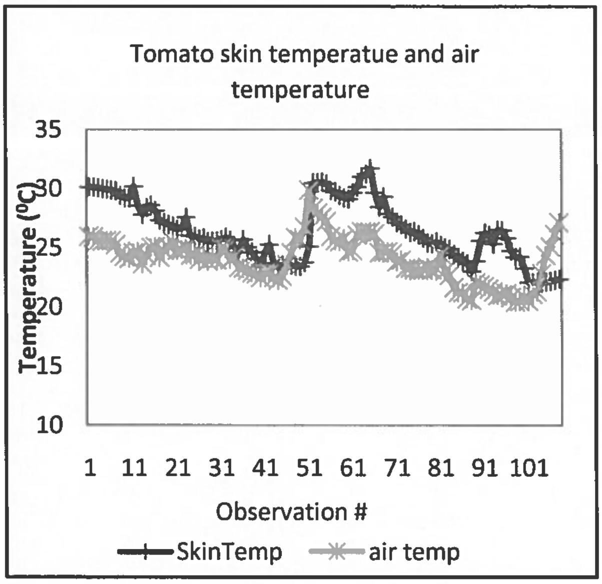

Appendix 7.3: Maps of in-cargo micro-climate produced in a GIS Environment

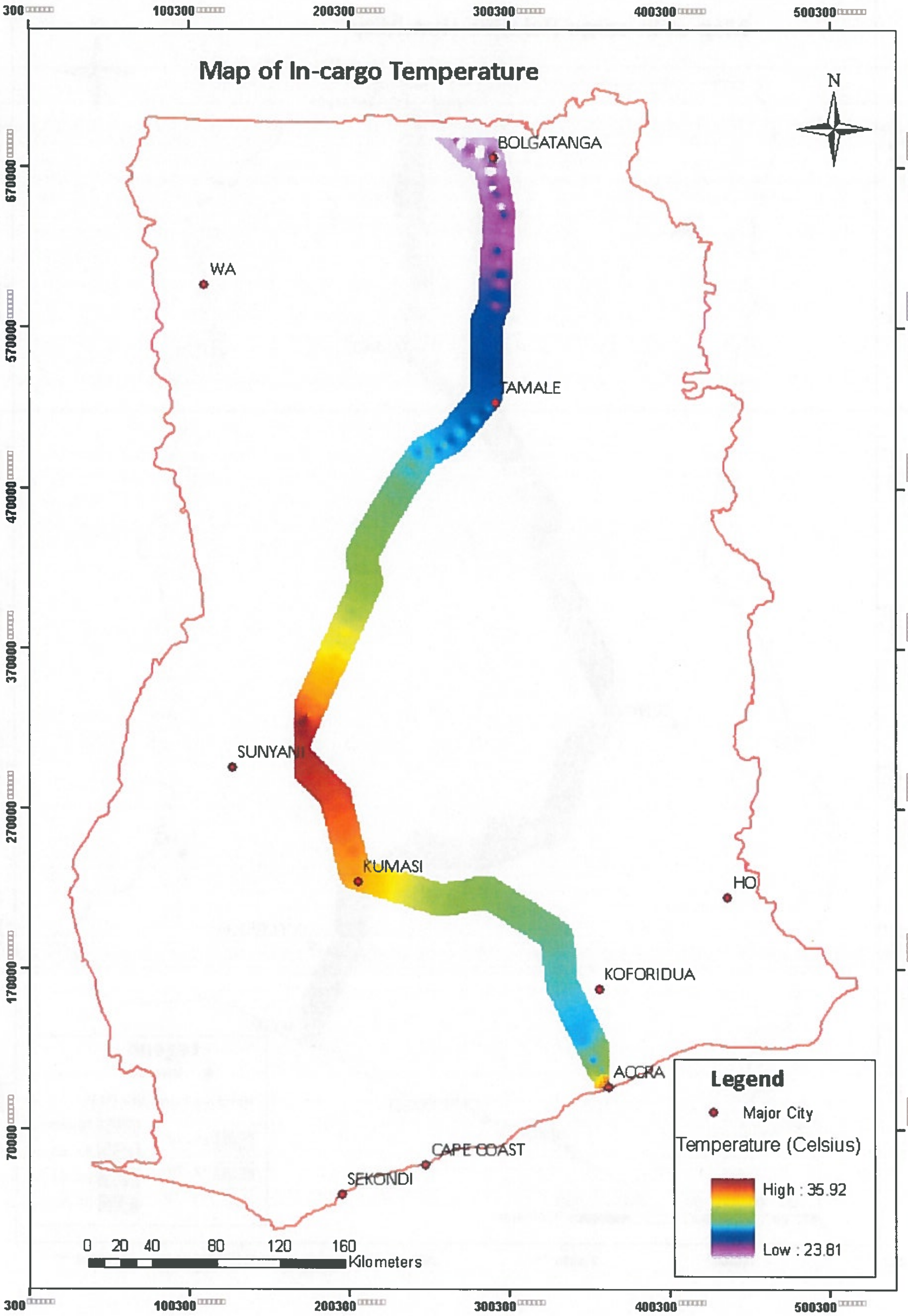

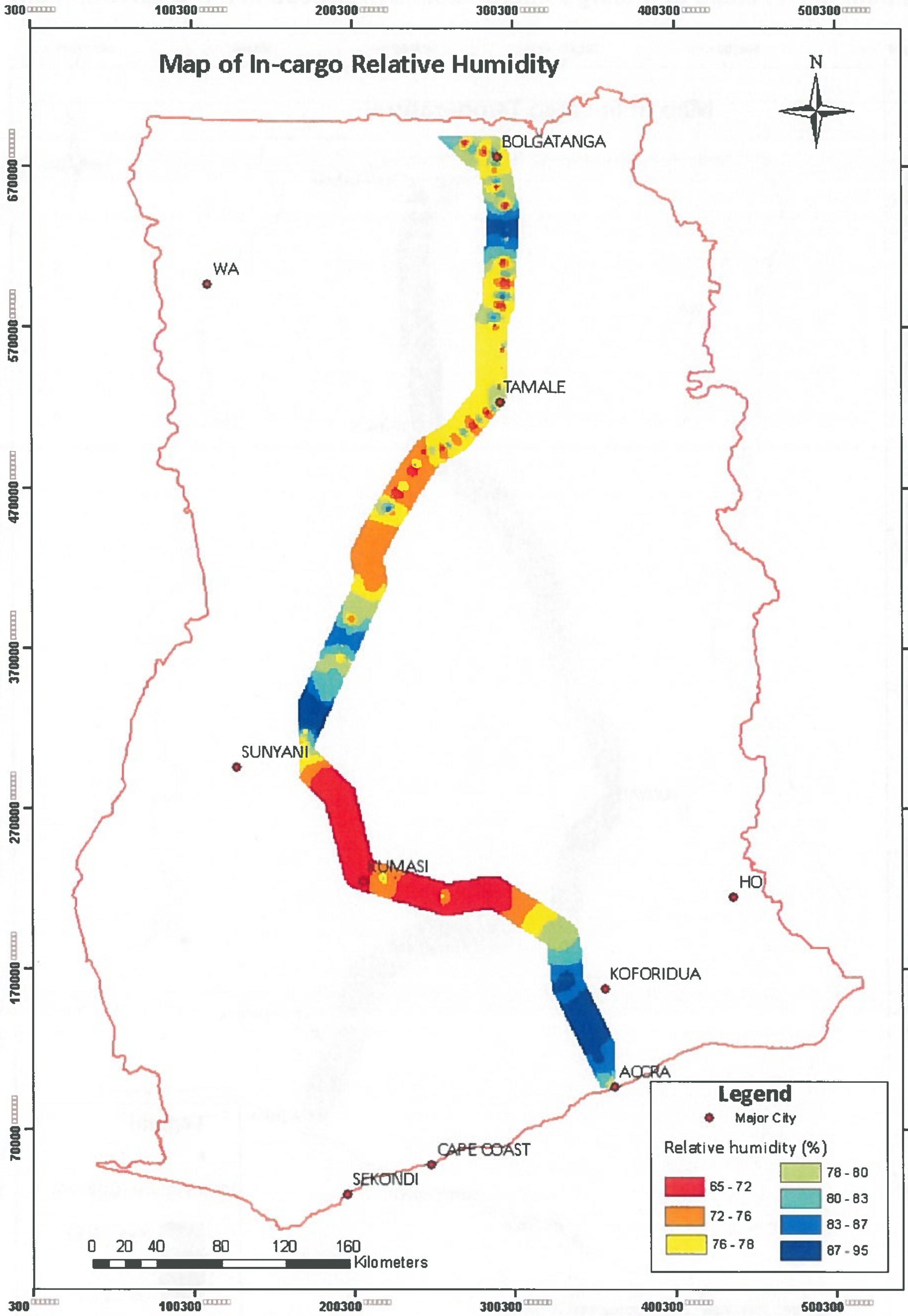
Map of In-cargo Relative Humidity
N
BOLGATANGA
WA
TAMALE
SUNYANI
KUMASI
HO
KOFORIDUA
ACCRA
CAPE COAST
SEKONDI
0 20 40 80 120 160
Kilometers
Legend
Major City
Relative humidity (%)
65 - 72
72 - 76
76 - 78
78 - 80
80 - 83
83 - 87
87 - 95
300
100300
200300
300300
400300
500300
670000
570000
470000
370000
270000
170000
70000

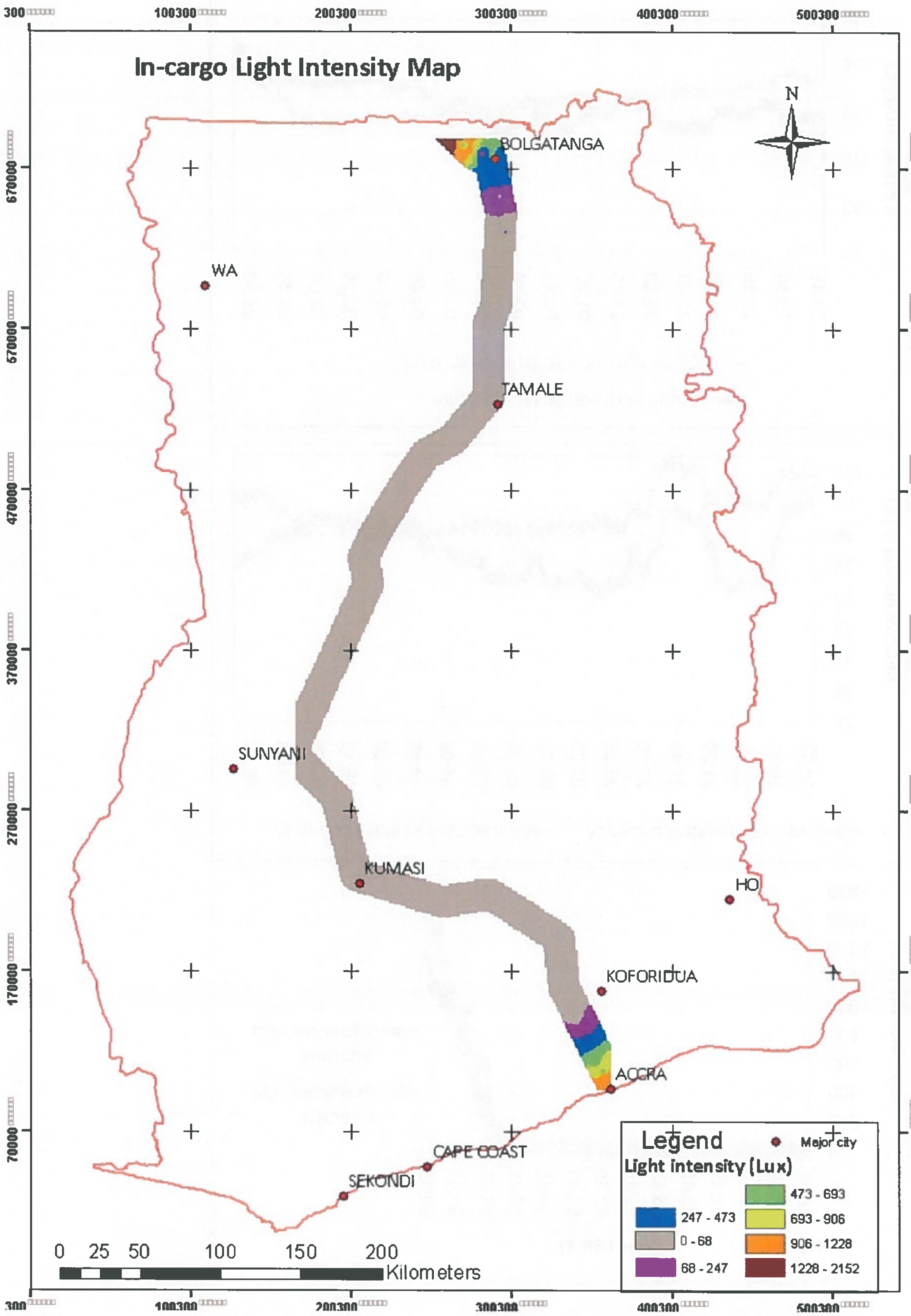
In-cargo Light Intensity Map
N
BOLGATANGA
WA
TAMALE
SUNYANI
KUMASI
HO
KOFORIDUA
ACCRA
CAPE COAST
SEKONDI
0 25 50 100 150 200 Kilometers
Legend
Major city
Light intensity (Lux)
247 - 473
0 - 68
68 - 247
473 - 693
693 - 906
906 - 1228
1228 - 2152
300
100300
200300
300300
400300
500300
670000
570000
470000
370000
270000
170000
70000

Appendix 7.4: Observed Versus Predicted results for the in-cargo micro-climate

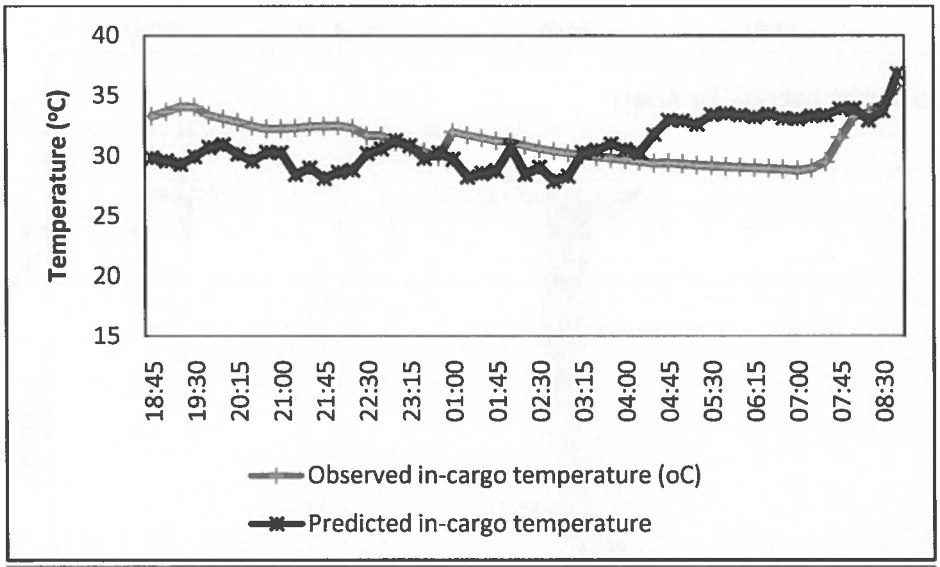

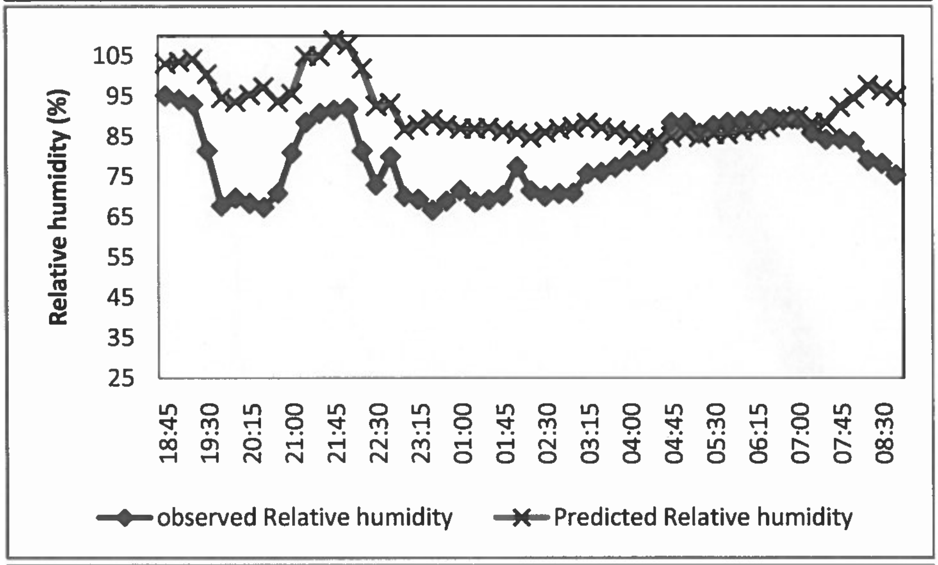

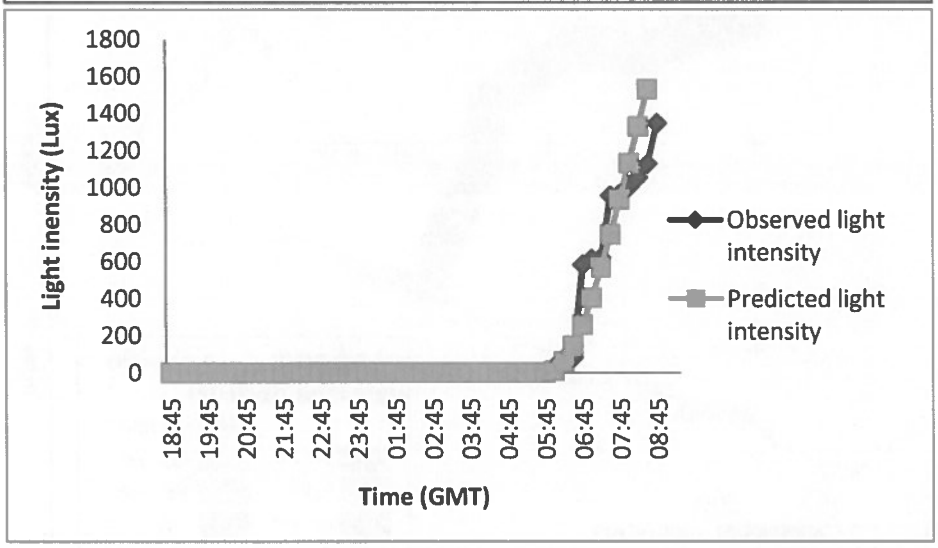

Appendix 7.5: Model for the Firmness Loss of Tomatoes during Dynamic Condition in Transport

Worked out exclusively for constant conditons

```
> R:=[F+L+RH>L+RH,k];
```

$$R := [L + RH < F + L + RH, k]$$

```
> odesnew(R);
```

$$\left[\left[\frac{d}{dt}F(t) = -k\,F(t)\,L(t)\,RH(t), \frac{d}{dt}L(t) = 0, \frac{d}{dt}RH(t) = 0\right], [F(0) = F0, L(0) = L0, RH(0) = RH0],\right.$$
$$[F(t), L(t), RH(t)], [L0 = L(t), RH0 = RH(t)], [L(t), RH(t)], 3,$$
$$\left.[L(t) = L0, RH(t) = RH0, F(t) = F0\,e^{(-RH0\,k\,L0\,t)}]\right]$$

```
> Fsol:=slis(dyna_sol[nana],F);
```

$$Fsol := F(t) = F0\,e^{(-RH0\,k\,L0\,t)}$$

```
> Fsol:=subs(RH0=aR+bR*RH,L0=aL+bL*L,Fsol);
```

$$Fsol := F(t) = F0\,e^{(-(aR + bR\,RH)\,k\,(aL + bL\,L)\,t)}$$

```
> pS:=mp([k=Arr(kref,Ea,20,T),F=rhs(Fsol)],parameters=[F0,kref,Ea,L,RH,aR,bR,aL,bL,T,t]);
pS := proc(F0, kref, Ea, L, RH, aR, bR, aL, bL, T, t)
local F, k;
    k := kref*exp(120.2790474*Ea*(1 / 293 - 1 / (T + 273)));
    F := F0*exp(-(aR + bR*RH)*k*(aL + bL*L)*t)
end proc
> plot(pS(5,.001,80,100,.5,.2,-.01,100,.02,20,t),t=0..100);
```